BOILING HEAT TRANSFER WITH LOW QUALITY STEAM

BY
THOMAS FRANK MARUCCI, LT. USCG

SUPERVISOR - ARTHUR E. BERGLES

MAY 21, 1965

BOILING HEAT TRANSFER WITH LOW QUALITY STEAM

by

THOMAS FRANK MARUCCI, Lieutenant, United States Coast Guard
B.S., United States Coast Guard Academy
(1959)

SUBMITTED IN PARTIAL FULFILLMENT
OF THE REQUIREMENTS FOR THE DEGREE OF
MASTER OF SCIENCE IN MECHANICAL ENGINEERING
AND THE PROFESSIONAL DEGREE
NAVAL ENGINEER
at the
MASSACHUSETTS INSTITUTE OF TECHNOLOGY
May, 1965

Signature of Author...
Department of Naval Architecture and
Marine Engineering, May 21, 1965.

Certified by ....
Thesis Supervisor

Accepted by ....
Chairman, Departmental Committee
on Graduate Students

[illegible]

[illegible]

Maurer II.

[illegible]

ABSTRACT

Boiling Heat Transfer with Low Steam Quality
Thomas Frank Marucci
Submitted to the Department of Naval Architecture and Marine Engineering on May 21, 1965, in partial fullfillment of the requirements for the Master of Science Degree in Mechanical Engineering and the Professional Degree, Naval Engineer.

Heat transfer for water and steam mixtures in a horizontal stainless steel tube under non-boiling, surface-boiling, and fully-developed boiling conditions was investigated.

Local heat transfer coefficients are presented for a limited range of flow parameters. Inside diameter of 0.2425 inch and a range of 14.4 to 78.5 L/D are considered. Exit pressure varied from 60 to about 72 psia for mass velocities from 5.9×10^5, to 2.38×10^6 lbs/hr ft^2. The range of steam quality covered was 0 to 44%. The majority of this data was taken at inlet temperatures of about 290°F. Heat fluxes ranged from 2×10^5 to 1.8×10^6 Btu/hr ft^2 and were limited by burnout conditions.

Heat transfer results for non-boiling and subcooled nucleate boiling are in agreement with previous investigations. Bulk boiling data is presented at the two lower flow rates. This data shows that as quality is increased, the local heat transfer coefficient also increases. This is indicated on the boiling curve as a shift toward lower wall superheat as quality increases. Similar results are indicated to a lesser degree with subcooled liquids at low values of subcooling. This appears to be due to the relatively large volume fraction of vapor created in the nucleate boiling process.

Experimental heat transfer coefficients obtained are considered to be in fair agreement with predicted values.

Thesis Supervisor: Arthur E. Bergles
Title: Assistant Professor of Mechanical Engineering

TABLE OF CONTENTS

		Page
TITLE		
ABSTRACT		
TABLE OF CONTENTS		
NOMENCLATURE		1
I	INTRODUCTION	4
II	PROCEDURE	6
III	RESULTS	12
IV	DISCUSSION OF RESULTS	17
V	CONCLUSIONS	26
VI	RECOMMENDATIONS	27
VII	APPENDIX	
	A. Experimental Apparatus	28
	B. Sample Calculations	34
	C. Summary of Data	39
	D. Bibliography	70
	E. Figures	73

NOMENCLATURE

A = surface area

A_c = test section cross section area

C_p = specific heat

D = diameter

E = voltage across the test section

E_s = shunt voltage

G = mass velocity

h' = enthalpy

h = heat transfer coefficient

I = current

k = thermal conductivity

L = heated length

p = pressure

q = heat transfer rate

q/A = heat flux

$(q/A)_i$ = heat flux at the inception of boiling

$(q/A)_{cr}$ = critical heat flux

$(q/A)_{FC}$ = forced-convection heat flux

R = electrical resistance

T = temperature

T_w = inside wall temperature

T_{ow} = outside wall temperature

V = velocity

w = mass rate of flow

x' = position along the test section measured from the inlet to the heated section

x = steam quality

ΔT_w = temperature drop through the tube wall

ΔT_{sat} = wall - minus - saturation temperature

ΔT_{sub} = saturation - minus - bulk temperature

μ = dynamic viscosity

σ = surface tension

ρ = density

ρ_e = resistivity

λ = latent heat of vaporization

Dimensionless Groups

Nu = Nusselt number = hD/k

Pr = Prandtl number = $C_p \mu / k$

Re = Reynolds number = GD/μ

Subscripts

b = bulk or mixed-mean conditions

BO = burnout condition

i = inlet bulk condition

exit = test section exit bulk condition

L = liquid condition

sat = saturation condition

t = tube

v = vapor condition

w = condition at heat transfer surface

INTRODUCTION

The current development of high performance heat-transfer equipment has stimulated a great amount of research in boiling heat transfer. Past studies of boiling heat transfer have been a factor in the development of nuclear reactors and rocket motors. Vaporization of the coolant is frequently desired, such as in the boiling-water reactor and bootstrap rocket engine.

There has been a vast amount of work in the field on forced convection-boiling heat transfer. Most of this has been concentrated on the prediction of burnout under given conditions of fluid, surface, and flow parameters. These studies have produced numerous correlations; the best of which can predict critical heat flux to about plus or minus 30% of experimental data.

Within the past ten years there has been an increase in the number of investigations designed to study heat transfer rates encountered in boiling heat transfer. The results of these studies have been presented in two basic forms. First, in the form of the boiling curve where heat flux is plotted versus wall superheat $(T_w - T_{sat})$. This has usually been utilized where the bulk fluid is subcooled, and indicates that heat flux can be represented as:

$$q/A = C\,(T_w - T_{sat})^n \qquad (1)$$

Other studies considered bulk boiling and present results that show

the local heat transfer coefficient (h) increasing as steam quality increases beyond a certain range. This range has been generally agreed upon as beginning at about 15% quality. As quality varies below this value h is constant.

Generally, when liquid flows through a heated tube, subcooled nucleate boiling can take place before the bulk of the fluid reaches its saturation point, if the impressed heat flux is high enough. The equilibrium thermodynamic quality would be zero in this subcooled region of flow, but the void fraction could be substantial, depending of course on the fluid properties and heat transfer rate. As flow proceeds down the tube the bulk of the fluid becomes saturated, net vapor generation commences. In this portion of the flow, the vapor generation can take place by additional nucleate boiling and/or by evaporation at the liquid-vapor interface. If the tube is long enough, it is possible to reach the point of 100% vapor.

This study was conducted to extend the fully-developed boiling curve in the region of bulk boiling and to determine what effect of variation in h with quality has on the boiling curve. It was also pointed out by Professor Bergles that non equilibrium voids created in subcooled region should have an effect on h.

The equipment used limits the study to low pressure, low flow rates and moderate heat fluxes. Fluid conditions included low subcooling and low steam quality. This study is particularly applicable in the development of evaporators for saline water conversion.

PROCEDURE

Operation and Data Taking

The experimental apparatus (Figure 1) used in this study was one already in operation at the M.I.T. Heat Transfer Laboratory. Only the test sections had to be fabricated to suit this study. Generally, the test sections had to be instrumented to provide means of determining local pressure and the temperature at the heat transfer surface. To obtain these measurements, pressure taps were located along the tube and thermocouples were placed on the outside wall of the test section. To insure that the outside wall was adiabatic, two guard heaters were used and maintained at a temperature equal to the tube wall temperature. A brief discussion of the experimental apparatus and a detailed discription of the construction of the test section is presented in Appendix A. A diagram of the heat transfer test section is shown in Figure 2. A preliminary investigation of critical heat flux was conducted to be able to predict the critical heat flux for the range of parameters to be studied. This was done primarily to avoid burnout of the elaborately instrumented heat transfer test sections. The test sections used to determine critical heat flux were not instrumented to obtain wall temperatures and were constructed with only one pressure tap located at the test section exit.

Prior to installation, the test section was given a final

internal cleaning with acetone. After installation, the entire test section was wrapped with insulation to minimize external heat losses. The loop was then filled with distilled water and all lines vented to remove air. The degassing operation was then initiated by heating the water in the degassing tank. With the water boiling, the loop water was heated and slowly sprayed into the top of the tank. Results from Reference (1) indicated that 20 minutes of such degassing reduced the dissolved-air content to approximately 1 c.c./liter. Two phase flow can influence system stability and recent studies have indicated that system instability can cause premature burnout. Air trapped in the system would provide a certain amount of compressibility. Reference (2) discusses system instabilities in more detail. After degassing, the heat exchanger cooling water was turned on to bring the system to normal temperature. The loop was then ready for operation, circulating distilled, deionized, and degassed water.

Critical heat flux data was obtained by increasing power gradually while maintaining constant flow rate, exit pressure, and inlet temperature. Critical heat flux was evaluated at the last recorded conditions prior to physical burnout of the test section. To vary exit quality conditions, inlet temperature was varied in subsequent runs.

The general procedure for taking heat transfer data was similar to that used for critical heat flux data. The major difference was that at each power level, while other conditions were maintained, the guard-

heater power was adjusted to the balance point, i.e., where the average guard-heater temperature (two-thermocouples) was the same as the average outer tube wall temperature (three thermocouples). These temperatures could not be kept exactly equal, but were maintained to within plus or minus 5°F of each other. At equilibrium, wall temperatures, fluid temperatures, pressures, pressure differences and test section voltage and current were recorded. The heat flux was then increased to the next level and the process repeated.

After the highest heat flux was completed, the power was reduced and the inlet temperature changed. Readings were then taken for a set of heat fluxes at a new inlet temperature.

The maximum attainable heat flux for any given run was determined by burnout except in one instance due to voltage limitations of the generators. The burnout heat flux was estimated from data presented in Reference (3) and from data taken in this study. It was desired to approach but not reach burnout. Temperature and pressure levels were largely determined by the system. Beginning at the lowest inlet temperature attainable, the inlet temperature was increased to about 20°F below the saturation temperature for the corresponding pressure. The exit pressure was maintained at 60 psia except at final runs where the minimum exit pressure obtainable for the desired flow rate exceeded 60 psia. This was attributed to the fact that choked flow conditions were present due to the large volume of vapor content in the test section.

Initial data taken with T.S.-1 and 2 was at relatively low values of heat flux and at low inlet temperatures. This was to obtain non-

boiling heat transfer data which is well correlated and hence serves as a check on instrumentation. By increasing the heat flux slowly it was possible to obtain data on the inception of nucleate boiling and to be able to trace the boiling curve in the transition region between non-boiling and fully-developed subcooled nucleate boiling.

At the higher heat fluxes with intermediate inlet temperatures the fully-developed subcooled nucleate boiling curve could be well established.

The final data was then taken with T.S.-2 at inlet temperatures near saturation. The inlet temperature was maintained below saturation at all times since the equipment did not allow determination of inlet conditions when net vapor existed at the inlet. This procedure provided data for bulk boiling over the quality range from 0 to 24%. To extend the data to higher steam qualities it was necessary to fabricate T.S.-3. T.S.-3 was constructed similar to T.S.-1 and 2 except that it was twice as long. The location of pressure taps and wall thermocouples for each test section is given in Appendix A. Due to inconsistent results as discussed later, T.S.-3 was modified by moving the thermocouples at the upstream locations to positions corresponding to L/D's at the downstream position of T.S.-2. One series of runs was conducted with this test section at $G = 1.19 \times 10^6$ and $T_i \simeq 290°F$. Accidental burnout and time limitations precluded going further with this study.

Data Reduction

All data reduction was done by hand calculation with the aid of a desk calculator. This included computation of local flow and heat transfer parameters, including flow rate, heat flux, wall superheat, bulk temperature or enthalpy as well as the dimensionless groupings Re, Nu, Pr, $Nu/Pr^{0.4}$. The mass velocity (G) was determined from the fluid flow rate and tube dimensions. The temperatures were converted from thermocouple emfs with NBS standard calibration. The heat input was obtained from the tube voltage and current (EI) and checked by the resistance and current, a third value was obtained from the mass flow, specific heat, and temperature rise. Values obtained by each were in excellent agreement and differed at most by 10%, but were usually within 5% of each other. The latter method was of no value when the exit temperature reached saturation. The average heat flux was calculated using the several values of heat input.

Heat transfer results were based on measurements of the outer wall temperature. A correction for temperature drop through the tube was made to first obtain the inner wall temperature. A modified form of the Krieth and Summerfield solution was used to obtain the necessary correction. This solution assumes an infinite cylindrical resistor, with heat transfer at the inner surface and an adiabatic outer surface. The final form of the equations as well as thermal-property information is given in Reference (1). The final form of the curve (ΔT_w versus I at various values of T_{ow}) is shown in (Figure 3). It should be noted that at high values of current, the wall temperature drop is extremely large. The data taken

in the last run (Table IV Series N Appendix C) points out the effects of this on the results. The wall temperature drop is so large that the inside wall temperature is actually reduced as the power level is increased. Results then indicate a substantial reduction in the degree of wall superheat. This leads to the conclusion that the equation for wall temperature drop may not produce accurate results at high values of current. High currents were reached with T.S.-2 as well, (Table IV Series F) but with a shorter test section the outside wall temperatures were also higher, hence, the effect was not as pronounced. At each thermocouple position, calculations were made to obtain the local heat-transfer results. The fluid bulk temperatures are based on a linear temperature gradient where data is for subcooled bulk fluid. Where net vapor existed, the bulk temperature is the saturation temperature for the particular local pressure. The local pressure was obtained graphically by drawing a smooth curve through the observed pressures at three locations. All fluid properties are based on these local bulk temperatures. With the saturation temperature (T_{sat}), the degree of subcooling ($\Delta T_{sub} = T_{sat} - T_b$) and the wall superheat ($\Delta T_{sat} = T_w - T_{sat}$) were available.

A sample set of calculations is shown in Appendix B. A tabulated summary of the data obtained is given in Appendix C.

RESULTS

Critical Heat Flux

Burnout data were required to set an upper limit on the heat flux that could safely be applied to the heat transfer section. This data is presented graphically in Figure 4, for $G = 1.19 \times 10^6$ lb/hr ft^2 ($V \simeq 5$ft/sec). Also plotted are data taken by Wessel (3)* for the same tube size with varying fluid velocity and a slightly larger tube with varying L/D($V \simeq 5$ft/sec). The data shows an increase in $(q/A)_{cr}$ as exit quality increases.

Heat Transfer Results

The non-boiling results of this study are presented in Figure 5, along with the line indicating McAdams (4) correlating equation. Data in Figure 4 were obtained for $G = 2.38$, 1.19 and 0.59×10^6 lb/hr ft^2 ($V \simeq 10$, 5, and 2.5 ft/sec). The span of Reynolds number also results from the bulk temperature variation. The data is consistently above that predicted by McAdams equation and can be represented by:

$$Nu = 0.017 \ Re^{0.85} \ Pr^{0.4} \qquad (2)$$

Subcooled nucleate boiling data is plotted in Figure 6. Figure 6 contains data at the same flow rates, $P \simeq 60$ psia, $L/D = 37.4$, and a range of subcooling from about 0 to 175°F. Three other curves are plotted to aid in describing the results.

First, the curve of $(q/A)_{FC}$ is the curve of heat flux versus wall superheat ($T_w - T_{sat}$) obtained from non-boiling prediction. This curve is based on $G = 1.19 \times 10^6$ lb/hr ft^2, and $T_{sub} = 109\text{-}183$°F, where

---

* Numbers denote reference listed in Bibliography

$(q/A)_{FC} = h(T_w-T_b) = h(T_w-T_{sat} + T_{sat} - T_b)$ and h is determined from properties at bulk temperature corresponding to the data using Eq (2).

Second, the curve of $(q/A)_i$ represents the locus of points at which surface boiling begins and where the heat flux departs from the non-boiling prediction. This is discussed in Reference (5) and is given by:

$$(q/A)_i = 15.60 \, p^{1.156} \, (T_w - T_{sat})^{2.30/p^{0.0234}} \qquad (3)$$

The curve plotted here is for p = 60 psia.

The third curve represents the mean line through data of Wessel for fully-developed subcooled nucleate boiling and was determined as indicated in Figure (7).

The data covers a range of flow conditions in the transition region from the inception of boiling to a point on the fully-developed boiling curve at which bulk boiling begins. As fully-developed boiling is reached, the data approaches an asymptote which agrees with Wessel's data. Figure (6) illustrates that in the transition region heat transfer rates are dependent on both flow rate and subcooling, and as the fully-developed boiling region is approached the dependence on flow rate and subcooling disappears.

Incipient boiling does appear to begin at the point predicted by the intersection of the incipient boiling curve and the non-boiling prediction.

Bulk boiling data is presented in Figures 8 and 9. Figure 8 shows data for L/D = 37.4, at the two lower flow rates for bulk boiling

(i.e., at points where the bulk fluid was at the saturation temperature). The data represents the range of steam quality from 0 to 24%. The fully-developed curve is again plotted for comparison. The data of Figure 8 to appear to follow the fully-developed boiling curve for the range of quality indicated.

Figure 9 contains data obtained with T.S. -2, 3, and 3 modified. The range of steam quality is extended to almost 40%, and data is plotted for varying L/D's. The data for a particular L/D can still be represented by a form of Eq. (1). But, as quality increases (represented by increasing L/D), the fully-developed boiling curves are shifted toward the lower wall superheat. The effect of quality seems to override the pressure effect, i.e., the lower pressure results in higher wall superheat.

Similar results appear in Figure 10 for data with subcooled boiling conditions. As L/D increases, at first, wall superheat increases, and then decreases. This appears to be independent of the degree of subcooling within the range covered in Figure 10 (T_{sub} = 30 - 150°F).

In an attempt to determine the effect of steam quality on heat transfer coefficient, Figures 11 through 14 show the experimentally determined heat transfer coefficient versus steam quality. Figure 11 contains data obtained with T.S. -2 for G = 0.59 and 1.19 x 10^6 $lb_m/hr\ ft^2$. The results indicate that heat transfer coefficients are dependent on heat flux, and flow rate alone in the range of steam quality. At

quantities above 10-15% the data appears to merge for each flow rate and the dependence upon heat flux disappears. The effect of flow rate is quite pronounced as would be expected. At lower flow rates the effect of quality on the local transfer coefficient becomes apparent at lower values of quality.

Figure 11 shows the results of T.S. -2 and 3 at $G = 1.19 \times 10^6$, and Figure 12 shows similar results for $G = 0.59 \times 10^6$. Data obtained from these test sections appears to be inconsistent. Results of T.S. -2 indicate an increase in h as flow proceeds downstream. If the data obtained from T.S. -3 is then compared with this, it would appear that h is relatively constant between 37.4 L/D and 57.9 L/D. Beyond that point h reaches a maximum and then decreases. Because of the inconsistency in the data, T.S. -3 was modified. The thermocouples located upstream on T.S. -3 (L/D = 57.9 and 64.1) were moved to positions which corresponded to the downstream thermocouple positions of T.S. -2 (L/D = 30.9 and 37.4).

Data taken with this test section is shown in Figure 13. Also plotted for comparision is data taken with T.S. -2 and 3 at $G = 1.19 \times 10^6$ lbs/hr ft^2. Data for each test section was taken at approximately equal values of heat flux and inlet temperature, in so far as data was available from the other test sections. Results of these last tests compare favorably with that obtained from test sections 2 and 3. The absolute values of h at corresponding L/D's are about the same. The only difference is that data from the modified test section shows an increase in h at the last thermocouple position instead of the decrease noted with T.S. -3

In order to compare the bulk boiling data with previous work in this area, Figure 14 shows the dimensionless ratio h/h_L versus the Martinelli parameter $(1/X_{tt})$, where the Martinelli parameter is defined by:

$$1/X_{tt} = (x/1-x)^{0.9} \ (\rho_L/\rho_v)^{0.5} \ (\mu_v/\mu_L)^{0.1} \tag{4}$$

h is the experimental heat transfer coefficient and h_L is the liquid heat transfer coefficient as given by the McAdams correlation. Also plotted here is Chen's F function and his prediction of h at parameters approximating the mean values for the data. The curve lies below the data at the lower L/D's of T.S. -2 , and 3 modified, but above the data for high L/D's of T.S. -3 and 3 modified. Chen's correlation is presented in a later section.

Figure 15 shows similar data at $G = .59 \times 10^6$ along with Chen's F function and his predition of h at parameters approximating the mean values for the data. Here Chen's F factor seems to divide the data for low L/D's and high L/D's. At the low flow rate Chen's prediction of h is higher than the experimental values.

DISCUSSION OF RESULTS

Critical Heat Flux

In the course of obtaining this data several interesting phenomena occurred. Although the primary intent of this study was to obtain heat transfer data, it is considered necessary to mention these items briefly.

First, the fact that $(q/A)_{cr}$ increased as much as 50% as the exit quality increased from 0 to about 25%. Previous studies in this area with subcooled fluid conditions at the exit have indicated that $(q/A)_{cr}$ decreases as the amount of exit subcooling decreases. The most recent studies show that as zero subcooling is approached $(q/A)_{cr}$ appears to level off and in some instances increases . This is indicated by the data of Wessel shown in Figure 4. One of the best known studies of burnout with exit quality is that of Lowdermilk (6). His results indicate that $(q/A)_{cr}$ is at a maximum when exit quality is approximately 20% depending on other flow parameters as well. The data did not cover the low range of exit quality. Hence, previous work indicated that, at a constant pressure and flow rate, $(q/A)_{cr}$ decreased as the exit subcooling decreased. Critical heat flux reaches a relative minimum, increases in the low range of exit quality to a relative maximum, and then falls off sharply. Bergles (1) also shows an increase in critical heat flux with an increase in quality up to 12%. Hence, the data presented here is in agreement with other studies. This critical heat flux is not as high as that attained with subcooled exit conditions. For more information in this area the reader is referred to recent studies by Loosmore and Skinner (7) on critical heat flux with subcooled boiling and by

Lopina (8) on critical heat flux with exit quality conditions.

Second, the actual location of burnout of the test section was not always at the exit. In fact, at exit quality near zero, and with exit quality about 25%, burnout did occur at the exit. Between these limits, the location of burnout was considerably upstream of the exit. In one run with exit quality approximately 13.6% burnout occurred at 18.7 L/D, while the overall tube dimensions in all runs was 41.4 L/D. Calculations indicate that the bulk fluid condition at the burnout location was slightly subcooled. This indicates that in the low range of exit qualities, exit conditions may not be the correct parameter to consider in determining critical heat flux. Lopina (8) and Waters, etal. (9) have also observed upstream burnout and discuss this in more detail. Waters' study shows that upstream burnout is reproduceable and not necessarily caused by instability.

Third, it was observed during operation that as the exit quality increased, the pressure drop from the test section exit to the exit plenum chamber became quite large. Hence, when measuring critical heat flux with net vapor generation, exit pressure must be determined at the test section exit and not in an exit plenum chamber. Results of this study indicated that there was essentially no pressure difference between these two locations at zero quality, but at 17.8% quality the pressure difference was approximately 12.5 psia at $G = 1.19 \times 10^6$ lbs/hr ft^2. To explain this it is necessary to give a brief discription of the method used to control the pressure.

The exit pressure level was controlled by means of a plug valve

downstream of the exit. At low values of heat flux, this valve was about midway between the fully opened and closed positions in order to maintain the desired pressure. As the heat flux was increased, and boiling conditions were reached, the exit pressure began to increase. This valve was then opened to reduce the pressure to the desired level. When bulk boiling conditions were reached, it was observed that pressure control was no longer possible, since the valve was wide open. As indicated previously, when the longer test section was used, pressure control was lost prior to obtaining the maximum heat flux for that series of runs. This then illustrates the choking effect that causes the pressure level to increase in the test section.

As the steam-water mixture leaves the test section, it enters a plenum chamber made up of 3/4 inch brass pipe. Expansion of the steam can take place immediately. The pressure drop encountered from the test section exit and the plenum chamber is the result of this rapid expansion.

Heat Transfer Results

Non-boiling data shown in Figure 5 plots consistently above the correlation of McAdams. The divergence appears to be primarily due to the radial property variation which is not properly accounted for in the correlation. This temperature difference effect is clearly demonstrated in Reference (10). In any case, Eq. (1) is not intended to be a generally valid correlation, but is merely indicated to represent the data.

Figure 6 shows the portion of the boiling curve from the inception

of boiling to the fully-developed boiling curve for three flow rates and two ranges of subcoolings. As indicated previously, inception of boiling did occur at the predicted value of wall superheat and heat flux. Beyond this point, the slope of the curve increases until fully-developed-boiling is reached. Using the data of Wessel to establish the fully-developed boiling curve (Figure 7), the data does approach this line as an asymptote. Hence, the subcooled data appears to be consistent with the work of previous studies.

At the onset of this study, Professor Bergles pointed out, that at high heat fluxes with low subcooling, the data appeared to be shifted from the fully-developed curve, toward lower wall superheats. It has already been mentioned, that fully-developed subcooled boiling data (Figure 10) show a change in wall superheat at different positions along the length of the tube. At the inlet, subcooled liquid velocity can be specified as V_1. As the fluid moves down the heated sections, surface boiling begins and non-equilibrium voids are formed. Therefore, the volume occupied by the liquid is reduced. In order that continuity be maintained, the liquid velocity must increase. Let this new velocity be V_2. As boiling becomes more vigorous along the tube, more volume is occupied by vapor and the liquid velocity continues to increase. This illustrates how the liquid velocity may increase along the length of the tube. With this in mind, and noting from Figure 6 that by increasing fluid velocity, fully-developed boiling is reached at higher values of heat flux.

If we consider three fluid velocities which do not differ by much, and determine the heat flux at which the lowest velocity reaches the

fully-developed boiling curve, it is clear that at this same heat flux, the wall superheat will be reduced at the two higher velocities. This example shows how the wall superheat can decrease at higher L/D's with subcooled liquids. This also indicates that the local heat transfer coefficient must increase in this range. The heat transfer coefficient is defined as:

$$h = (q/A) / (T_w - T_b) \tag{5}$$

As long as the bulk fluid is subcooled, the bulk temperature is increasing along the direction of flow. If $(T_w - T_{sat})$ decreases as indicated previously and T_{sat} decreases with pressure, then T_w must also be decreasing. As a result, $(T_w - T_b)$ must decrease and the heat transfer coefficient increases due to the presence of void fractions. This explains the trend toward lower wall superheat in data at high L/D's as shown in Figure 10.

Bulk boiling data (Figure 9) also shows a reduction in wall superheat with increasing L/D. Bennett, etal. (11) presents a discussion on the effect of net vapor generation, similar to the discussion above on the effects of void fraction on fluid velocity. This explains the lower wall superheats obtained at the exit of the test section. In the region of bulk boiling where the bulk temperature is the saturation temperature, a decrease in wall superheat means an increase in h for a specified heat flux. Therefore, wherever net vapor exists, there is an increase in the local heat transfer coefficient.

Now, consider a section along the tube where the bulk fluid is slightly subcooled. As flow proceeds down the tube the bulk fluid approaches

saturation conditions. The rate at which bubbles nucleate at the surface decreases since the fluid velocity is greater. At the same time, the bubbles, which have just departed the surface, do not collapse and the volume fraction of vapor remains nearly constant. Then, the fluid velocity will also remain constant and the degree of wall superheat predicted by the boiling curve will not change. Therefore, in this region near zero quality, the heat transfer coefficient is relatively constant as well. Further along the heated section, net vapor generation continues by means of surface boiling and/or evaporation at the liquid vapor interface. At this point, the fluid velocity begins to increase again and continues to increase until the test section exit is reached. This appears to explain the data of Figure 9, as well as that of Figure 11.

Figure 12 with data of T.S. -2 and 3 at $G = 1.19 \times 10^6$ lbs/hr ft^2 shows the discrepancy in the data obtained from these two test sections. Data obtained with T.S. -3 shows that, as x increases, h reaches a maximum and then decreases. This could not be explained adequately. Considering data for an approximate equal heat flux for the two test sections, there also appears to be a discontinuity in the data between $L/D = 39.4$ and 57.9. The value of h increases as L/D increases to 39.4, but apparently there is no further increase in h to $L/D = 57.9$. Beyond this point, h reaches its maximum value and decreases. Results for $G = 5.9 \times 10^5$ lbs/hr ft^2 shown in Figure 12 are similar.

It was expected that data obtained with T.S. -3 modified would resolve this discrepancy. Figure 13 shows data for one flow rate and one

value of heat flux for T.S. -2, 3, and 3 modified. The results of this show that the absolute magnitudes of h remained about the same. The only difference which did appear consistently was that at high L/D's, h increased rather than decreased. The heat transfer coefficient then showed and increase over the first half of the T.S., then remained a relatively constant value, and finally increased again near the exit. One possible explanation is; at the lower L/D's flow conditions had just reached the point at which the void fraction is nearly constant. Over a short range beyond this point, h is constant with x. If this were true, the results as indicated in Figure 11, are misleading and quality does not significantly affect h until it reaches a value of about 20%.

Another method of evaluating the data would be to draw the mean line through the data from both test section. It is uncertain which data, if any, is actually incorrect. If this were done in Figure 12, it would indicate the effect of quality becomes apparent at about 15%, but its overall effect would not be as great as indicated in Figure 11.

Figures 15 and 16 show the same data on another set of coordinates, h/h_L versus $1/X_{TT}$. Dengler and Addoms (12) were the first to use these coordinates in evaluating this type of data. Here h_L is defined as the conventional liquid heat transfer coefficient determined by McAdams' correlation. They proposed a correlation for two phase heat transfer coefficients in terms of $1/X_{TT}$ (the Martinelli parameter) and an F factor to account for the degree of nucleate boiling present. As the fluid progresses into the annular flow regime, with continuiously increasing steam quality, the increased velocity of the two phase mixture induced by the vaporization process suppresses the nucleate boiling process. Beyond this point the heat transfer coefficient becomes governed by the forced convection process.

With this in mind Chen (13) proposed the following correlation for the two phase heat transfer coefficient:

$$h = h_{mic} + h_{mac} \qquad (6)$$

where h_{mic} is the microconvective portion due to the boiling mechanism and hence dependent on liquid and bubble parameters:

$$h_{mic} = .00122 \frac{k_L^{0.79} \; C_{pL}^{0.45} \; \rho_L^{0.49} \; g_c^{0.25}}{\sigma^{0.5} \mu_L^{0.29} \lambda^{0.24} \rho_v^{0.24}}$$

$$X \; (\Delta T_{sat})^{0.24} \; (\Delta P_{sat})^{0.75} \; S \qquad (7)$$

and h_{mac} is the macroconvective given by:

$$h_{mac} = h_L \; F \qquad (8)$$

Again h_L is given by McAdams' equation. F is a function of the Martinelli parameter and is defined as the ratio of the two phase Reynolds number to the liquid Reynolds number. S is called the suppression factor and approaches unity at zero flow rate, and zero at infinite flow rate. Gouse (14) suggests that this suppression factor should go to zero much sooner and thus acknowledge the possibility of total suppression of nucleation at finite Reynolds number. Both S and F are presented graphically in Reference (13).

Chen restricts the applicability of this correlation to systems with annular or annular mist flow in vertical geometries. This

correlation successfully predicts the data of numerous independent studies to within plus or minus 15%, and seems to be one of the best available. Gouse (14) also states that there is no reason why it should not apply to annular flow in horizontal tubes.

Data obtained with thermocouples at the top and bottom of the tube wall, at the same location along the length, produced no indication of stratification. Thermocouples indicated that the temperature difference obtained in all cases was less than the accuracy of the measurement. Also, the greater temperature fluctuated between the top and bottom. With this in mind Chen's correlation is considered a suitable means of checking the data.

As noted earlier Chen's prediction seems to plot between the data for high and low L/D's indicating that the difference can be considered as scatter in the data. It must be noted, that scatter of such a consistent nature is unusual.

CONCLUSIONS

Critical Heat Flux:

The critical heat flux increased as much as 50% as exit quality was increased from 0 to 25%.

Heat Transfer

1. The local heat transfer coefficient, obtained at subcooled boiling conditions, does appear to increase due to the presence of voids formed during the boiling process.
2. As bulk fluid approaches saturation conditions the local heat transfer coefficient is constant over a low range of steam quality. The extent of this range increases as the flow rate increases.
3. For the flow rates considered in this investigation, the local heat transfer coefficient shows a significant increase as quality is increased beyond 15%.
4. Chen's correlation appears to be fairly accurate in the low range of steam quality, but it's accuracy improves as quality increases and nucleate boiling is suppressed.

RECOMMENDATIONS

Critical Heat Flux

1. When bulk fluid conditions at the exit contain vapor, the exit conditions must be determined by the pressure at the test section exit rather than the pressure in an exit plenum chamber.
2. Since upstream burnout is possible with exit quality conditions, and stable flow, it may be of interest to determine if some parameter, other than exit quality might give a more meaningful indication of the results.

Heat Transfer

1. Additional experiments should be conducted with test sections similar to T.S. -3 and instrumentation covering a greater portion of the test section. This is suggested to see if there is actually a region along the test section where the local heat transfer coefficient is constant.
2. Additional study of heat transfer coefficient in the low quality range is still required, in order to develope a more accurate prediction in the range where heat transfer rates are dependent on the combined effects of boiling and convective heat transfer.

APPENDIX A

EXPERIMENTAL APPARATUS

Flow Loop and Power Supply

The flow loop used in the experimental program was one already in operation at the M.I.T. Heat Transfer Laboratory. This facility is shown schematically in Figure 1. It was a closed loop system in which all components are of corrosion resistant materials. The system contained the main circulating pump, an accumulator, the test section line with parallel flow meters, preheater, test section and its instrumentation, the bypass line, and a heat exchanger utilizing city water. Auxiliary equipment included a fill pump, supply tank, degassing tank, and a continuous demineralizer. The test section power was supplied by an a.c. motor - d.c. generator set. A discription of the major components follows. More detailed information is given in Reference (1).

The main circulating pump was a two-stage, turbine-type pump driven by a 3hp induction motor. It provided a head of 250 psi at 3.6 gpm. A bladder type accumulator, pressurized with nitrogen, located at the pump exit served to damp out pressure fluctuations. The ball valve in the by-pass line was used to control the by-pass flow rate and pressure, which in turn determined the pressure in the test-section line. The test section line contained a Fischer-Porter flow meter and a set of preheaters in series. There are four 5kw preheaters plus an additional 5kw emersion unit fabricated in a 3 inch copper tube and provided with 0 to 100% control by a Powerstat auto-transformer. This arrangement allowed varying preheat from 0 to 25kw, one being variable and the other allowing increments of 5kw each.

The test section power was supplied by motor-generators. The generators were driven by 440 volt, 3 phase synchronous motors. Two 36kw d.c. generators, each nominally rated at 12 volts and 3000 amps were connected in series. The generators were provided with water cooled shunts in parallel with the test section which allowed them to be run open circuited at the test section for starting, or after burnout.

Instrumentation

Instrumentation was available for reading pressure levels, differential pressure, temperature, test section flow rate and test section voltage and current. Pressure levels were read on bourdon-tube gages as shown in Figure 1. At the test section inlet and exit were 200 and 100 psi test gages with an accuracy of plus or minus 1/4% of full scale.

Test section flow rate was determined from the larger flowrater meter which had interchangable tubes and floats. The ranges covered are 20-160, 35-400, and 140-1360 lb/hr. All units were calibrated as installed in the system.

The power supplied to the test section was obtained from the test section voltage and current. The voltage was read directly on a Weston multiple-range d.c. voltmeter with a specified accuracy of plus or minus 1/2%. The current was determined from a standard shunt with a calibration of 60.17 amp/mv.

All temperatures were measured with copper-constantan thermocouples made from 30 gage duplex wire. The fluid bulk temperature at the inlet

and exit of the test section was measured by inserting thermocouples directly into the fluid using conax fittings with lava sealants. Methods of measuring wall temperature are described later. The output voltages of the thermocouples and the shunt were displayed on a continuous recorder. The recorder was a Brown, single channel instrument having ranges of 0-6, 5-11, 10-16, 15-21, and 20-26 mv.

The manometer system used to measure differential pressure consists of two Meriam 60 inch U-tube manometers, manifolds and valves, and connecting lines of rubber hose. The system is designed to read a maximum of 10 pressure differences with either one or two reference points on either manometer. One manometer was filled with mercury which gave a maximum range of approximately 25 psi. The other manometer contained an oil with a specific gravity of 2.00 which allowed a maximum pressure difference of approximately 2 psi. A typical test section with three pressure taps is shown in Figure 2. The pressure drop from the reference "A" located at the inlet, to points 2, and 3 could be read on either the mercury or oil manometers depending on the magnitude of the pressure drop. The two pressure gages were connected to the inlet and exit to give the pressure level and a check on the pressure drop. Vents were included so that all lines could be purged of air.

Measurement of Tube-Wall Temperature

The most difficult problem in any heat transfer experiment is the measurement of the temperature of the heat transfer surface. The basic method of measuring tube wall temperature is described in Reference (1).

The method used here was as follows:

Heated shields constructed of standard aluminum tubing, with threadlike grooves cut into the outer wall, were wrapped with insulated Chromel A-26 wire. Spacers fabricated from aluminum served to hold the shield in place.

Power was suppled in the Chromel heating coil by a 110 VAC supply which is stepped down to about 25 volts by a Stancor filament transformer. The power to each shield is controlled by a Powerstat. This arrangement permits fine control of shield heating.

A layer of Scotch Electrical tape Number 27 was wrapped around the tube at each thermocouple location. The measuring junction was then bound radially around the tube with another layer of tape. Thermocouples were also taped to the inside of the shield. Sufficient length of all thermocouples were left inside the shield to avoid conduction errors. The space between the shield and tube was filled with asbestos fiber. Precautions were taken to insure the shield was electrically insulated from the test section.

Power to the shields is adjusted until the shield thermocouples and the tube wall thermocouples within the shield section indicate approximately equal EMF.

Test Section

The test section was constructed from 304 stainless steel tubing with an inside diameter of 0.2425 inch. Brass bushings were cut from 3/4 inch round stock. Holes were drilled for the test section. The bushings were then sweated to the tube with silver solder. Holes 0.099

inch were then drilled in the bushings for pressure taps. These holes did not penetrate the test section. A number 75 drill (0.021 inch) was used to drill the pressure tap hole. Beryllium copper pressure tap tubes (2mm ID) were then set in the bushings and soft soldered in place. The inside of this tube was filled with milk of magnesia to prevent the tap being plugged. With this completed, the milk of magnesia could then be removed.

An additional pressure tap was placed near the center of the test section. Here a short stainless steel tube was first filled with milk of magnesia and then silver brazed to the test section. Excess braze was then filed away to give a very small fillet at the test section. The milk of magnesia was removed and the pressure tap hole drilled (0.021 inch) through the test section. Any burrs inside the tube were removed with fine emery cloth and pieces of steel wool pushed through the tube.

Thermocouples were then attached to the test-section wall as described previously. Thermocouples were located at four positions along the length. At two locations the thermocouples were placed perpendicular to the tube axis, and the lead wires wrapped around the tube and taped in place. At the other two locations, thermocouples were again placed perpendicular to the tube axis, but at each of these positions two thermocouples were used, one on the top of the tube and the other at the bottom. This set up was intended to detect stratification.

The guard heaters were then assembled onto the test section. After the first guard heater was in place a section of 0.099 inch OD tubing was placed over the center pressure tap and soft soldered to the stainless steel tube to extend this pressure tap. A diagram of this test

section is shown in Figure 2.

T.S. -1 and 2 were identical in construction. Accidental burnout early in this investigation is the reason for this. The location of pressure taps and wall thermocouples is indicated below.

T.S. 1 and 2

Calming length 6 in.

Heated length 10 in.

Center pressure tap at 27.3 L/D

No.	Distance to thermocouples
1	14.4 L/D
2	23.7
3	30.9
4	39.4

T.S. 3

Calming length 6 in.

Heated length 20 in.

Center pressure tap at 45.5 L/D

1	57.9 L/D
2	64.1
3	72.4
4	78.5

T.S. 3 modified

Calming length 6 in.

Heated length 20 in.

Center pressure tap at 45.5 L/D

1	30.9 L/D
2	39.4
3	72.4
4	78.5

APPENDIX B

SAMPLE CALCULATION

1. Calculation of heat input to the test section:

   (a) from the current and voltage measurements

   $q_a = 3.413 \; EI = 3.413 \; (60.17) \; E \; E_s$

   $= 205.36 \; E \; E_s$ Btu/hr

   E and E_s were measured values.

   (b) from current and resistance

   $q_b = 3.413 \; I^2 \; R = 1.236 \times 10^4 \; E_s^2 \; R$

   $R = \rho_e \; L/A_c$

   For T.S. -1 and 2 $L = 10/12$ ft,

   $A_c = (\pi/4) \; (ID^2 - OD^2)/144 = 2.115 \times 10^{-4} \; ft^2$

   $R = 0.394 \times 10^4 \; \rho_e$

   ρ_e was determined from Reference (1) as a function of the tube temperature. The tube temperature is given by:

   $$T_t = T_{ow} - (\Delta T_w/2)$$

   ΔT_w was determined from Figure 2 and is a function of T_{ow} I. T_{ow} was measured by means of thermocouples converted with N.B.S. tables.

   (c) from mass flow rate and bulk temperature change

   $q_c = w \; C_p \; (T_{exit} - T_i)$

   T_{exit} and T_i as well as all other temperatures was obtained as indicated above for T_{ow}.

A sample set of data and calculations are shown on the following pages.

Data for Run A-8

E	E_s	P_i	ΔP_{i-2}	ΔP_{i-3}	P_3	T_i		T_{exit}	
v	mv	psig	in-oil	in-oil	psig	mv	°F	mv	°F
12.65	18.62	46.0	0.9	8.9	44.6	0.52	56	3.68	189

T_A*	T_B*	T_{ow-1a}**		T_{ow-1b}**		T_{ow-2}	
mv	mv	mv	°F	mv	°F	mv	°F
11.36	11.30	11.37	461	11.29	458.7	11.40	462

T_C*	T_D*	T_{ow-3}		T_{ow-4a}**		T_{ow-4b}**	
mv	mv	mv	°F	mv	°F	mv	°F
11.48	11.43	11.66	470.7	11.51	456.7	11.43	463

$$q_a = 12.65\ (18.62)\ (205.36) = 48122 \text{ Btu/hr}$$

$$q_b = 1.236 \times 10^4\ (18.62)^2\ 1.119 \times 10^{-2} = 47750 \text{ Btu/hr}$$

$$I = 60.17\ (18.62) = 1120 \text{ amps } \& \ T_{ow} = 465\ ^{o}F$$

then Figure 2 gives $\Delta T_w = 115\ ^{o}F$

$$T_t = 465 - 57.5 = 407.5\ ^{o}F \text{ and } \rho_e = 2.84\ (10^{-6}) \text{ ohm ft}$$

$$R = 1.119 \times 10^{-2} \text{ ohms}$$

$$q_c = 364\ (189 - 56) = 48412 \text{ Btu/hr}$$

$$q = (q_a + q_b + q_c)/3 = 48093 \text{ Btu/hr}$$

2. Heat transfer surface area $A = \pi(ID)\ L = 0.0529\ ft^2$

3. Average heat flux $q/A = 48093/ .0529 = 9.159 \times 10^5$ Btu/hr ft^2

4. The change in enthalpy through the test section is

$$\Delta h' = q/w = 135 \text{ Btu/lb}_m$$

5. The change in bulk temperature from inlet to any position along the

---

* T_A, T_B, T_C and T_D denote guard heater temperatures.

** The a and b indicate temperatures at the top and bottom of the tube respectively.

tube is given by:

$$T_b = (T_{exit} - T_i) \quad x'/ L$$

6. The pressure at any point along the tube was obtained graphically as indicated earlier.
7. Entering the steam tables with the local pressure, the saturation temperature, the saturated liquid enthalpy and the latent heat of vaporization were obtained.
8. All fluid properties at each thermocouple position were obtained at the local bulk temperature. These include C_p, k, ρ, μ, and P_r.
9. At each position the following values were obtained as indicated above.

L/D	x'/L	T_{ow}*	ΔT_w	T_w	$P_{x'}$	$T_{sat_{x'}}$
14.4	.35	a 461.0 b 458.7	115	345.0	60.2	292.9
23.7	.575	462.0	115	347.0	59.9	292.6
30.9	.75	470.7	115	355.7	59.6	292.3
37.4	.906	a 465.7 b 463.0	115	349.3	59.4	292.1

---

* The temperatures at a and b were averaged to give the outside wall temperature at these locations.

L/D	ΔT_b	$T_{b_{x'}}$	ΔT_{sat}	ΔT_{sub}	$(T_w - T_b)_{x'}$
14.4	46.3	102.3	52.1	191.6	242.7
23.7	76	132	55.4	160.6	215.0
30.9	99	155	63.4	147.3	200.0
37.4	119.9	165.9	57.2	126.2	183.4

10. The local value of h was not calculated for subcooled boiling data, but was determined for non-boiling and bulk boiling data as shown:

$$h = (q/A) / (T_w - T_b)$$

11. Nu and Re were determined for non-boiling data as well as the ratio $Nu/Pr^{0.4}$.

$$Nu = hD/k = (h/k)\ (0.0202)$$

$$Re = GD/\mu = 2.404 \times 10^5 /\mu \qquad @\ w = 364\ lb_m / hr$$

$$Pr = C_p \mu/k$$

Pr is tabulated as a function of temperature in Reference (15) with the other properties for water.

12. Bulk boiling data included some additional calculations as indicated:

(a) local enthalpy $h'_{x'} = h'_i + \Delta h'_{x'}$

where $\Delta h'_{x'} = (h'_{exit} - h'_i)\ x'/L$

NOTE: When this value exceeded the value of saturated liquid enthalpy, net vapor was present. The local quality was calculated using the local enthalpy, saturated liquid enthalpy and latent heat of vaporization.

(b) Evaluation of the Martinelli parameter required values of μ and ρ for steam. μ_v was obtained from Reference (16) and

ρ_v was obtained from the steam tables. The Martinelli parameter was then calculated for each data point at which net vapor was present. The Martinelli parameter is defined as:

$$1/X_{TT} = \left(\frac{x}{1-x}\right)^{0.9} (\rho_L/\rho_v)^{0.5} (\mu_v/\mu_L)^{0.1}$$

(c) To obtain the ratio h/h_L, the liquid heat transfer coefficient (h_L) was calculated at each of these data points with McAdams equation:

$$h_L = 0.023\ (k/D)\ Re^{0.8}\ Pr^{0.4}$$

This equation was used because it provided a means of comparing the data with Chen's work in this field. His value of h_{mac} is equal to h_L, as determined above, multiplied by his F factor.

A summary of the data is contained in Appendix C.

APPENDIX C

SUMMARY OF DATA

			Page
Table	I	Burnout Data	40
Table	II	Non-boiling Data	41
Table	III	Subcooled Nucleate Boiling Data	45
Table	IV	Bulk Boiling Data	55
Table	V	Range of Variables	69

TABLE I

BURNOUT DATA

$D = 0.2425$ inch $L = 10$ inches $L/D = 41.4$ $V = 5$ ft/sec

RUN	P_{exit} psia	$(q/A)_{cr} \times 10^{-6}$ Btu/hr ft^2	$(h'_{exit} - h'_{sat})$ Btu/lb	$(h'_{BO} - h'_{sat})$ Btu/lb
1	30	1.325	20	*
2	56	1.42	65	47
3	52	2.135	241	*
4	40	1.18	52	-30.4
5	42	1.568	109	1.1
6	45	1.638	160	20.1
T.S.2	72	1.95	296.4	*

* Burnout occured at the exit

TABLE II

NON-BOILING DATA

L/D	RUN	$Nu/Pr^{0.4}$	$Re(10^{-3})$	RUN	$Nu/Pr^{0.4}$	$Re(10^{-3})$	RUN	$Nu/Pr^{0.4}$	$Re(10^{-3})$
Series A									
14.4	1	33.5	6.97	2	32.8	7.75	3	36.7	9.00
23.7		34.1	7.00		32.65	8.30		43.6	10.5
30.9		36.6	7.10		37.4	8.85		46.4	11.7
37.4		37.6	7.20		34.4	9.20		54.8	12.9
Series B									
14.4	1	66.9	23.0	2	80.8	24.1	3	140	41.1
23.7		69.0	23.5		80.4	24.9		143	42.6
30.9		67.1	23.9		80.3	25.9		147	43.4
37.4		71.7	24.4		79.6	26.3		149	43.6
14.4	4	125	24.75						
23.7		122	26.0						
30.9		118	27.5						
37.4		123	29.75						

TABLE II CON'T

Series C

L/D	RUN	$Nu/Pr^{0.4}$	$Re(10^{-3})$	RUN	$Nu/Pr^{0.4}$	$Re(10^{-3})$	RUN	$Nu/Pr^{0.4}$	$Re(10^{-3})$
14.4	1	105	23.8	2	103	24.9	3	91.8	23.7
23.7		105.8	24.2		111.5	26.3		90.0	24.2
30.9		100	24.9		112	27.2		91.6	24.7
37.4		100	25.4		113	28.5		96.5	25.0
14.4	4	86.3	26.4						
23.7		89.2	27.8						
30.9		91.0	28.4						
37.4		91.8	29.2						
Series D									
14.4	1	97.8	27.5	2	126	36.0			
23.7		92.5	28.1		124.5	32.0			
30.9		87.9	28.2		121.3	33.0			
37.4		84.4	28.7		122.3	34.4			

TABLE II CON'T

Series G

L/D	RUN	$Nu/Pr^{0.4}$	$Re(10^{-3})$	RUN	$Nu/Pr^{0.4}$	$Re(10^{-3})$	RUN	$Nu/Pr^{0.4}$	$Re(10^{-3})$
14.4	1	67	17.0	2	70.0	18.0	3	78.4	19.6
23.7		71.5	18.4		74.4	19.7		85.3	22.0
30.9		74.1	19.6		77.0	20.8		89.0	23.8
37.4		77.3	20.6		83.8	22.4		95.2	25.8
14.4	4	86.1	20.0						
23.7		94.5	23.2						
30.9		104.8	25.8						
37.4		114.5	29.0						

TABLE II CON'T

Series H									
L/D	RUN	$Nu/Pr^{0.4}$	$Re(10^{-3})$	RUN	$Nu/Pr^{0.4}$	$Re(10^{-3})$	RUN	$Nu/Pr^{0.4}$	$Re(10^{-3})$
14.4	1	160	46.5	2	166.7	48.0	3	157.2	49.9
23.7		168	48.2		166.0	49.6		175	52.0
30.9		148	49.4		159.8	50.6		168.8	53.6
37.4		153.4	50.0		163.8	52.2		172.2	55.2
14.4	4	180	49.9						
23.7		182	52.6						
30.9		176.5	55.2						
37.4		184	57.0						
Series I									
14.4	1	22.6	4.84						
23.7		22.9	4.99						
30.9		23.8	5.04						
37.4		26.7	5.11						

TABLE III

SUBCOOLED BOILING DATA

Series A

L/D	RUN	$q/A \times 10^{-6}$ Btu/hr ft^2	ΔT_{sat} ^oF	ΔT_{sub} ^oF	RUN	$q/A \times 10^{-6}$ Btu/hr ft^2	ΔT_{sat} ^oF	ΔT_{sub} ^oF
14.4	4	.62	27.4	211	5	.454	21	219
23.7			34.3	191			22	207
30.9			41.0	173			23	193
37.4			39.6	158			23	183
14.4	6	.53	28	214	7	.765	42.8	200
23.7			29	197			48	175
30.9			33	183			58	154
37.4			30	171			51	137
14.4	8	.915	52	191	9	.954	51.5	187
23.7			55	150			55.3	155
30.9			63.7	137			62.3	131
37.4			57.5	116			57.3	109

TABLE III CON'T

L/D	RUN	q/Ax 10^{-6} Btu/hr ft^2	ΔT_{sat} ^oF	ΔT_{sub} ^oF	RUN	q/A x 10^{-6} Btu/hr ft^2	ΔT_{sat} ^oF	ΔT_{sub} ^oF
Series B								
14.4	5	.468	39.1	114	6	.918	43	96
23.7			42	100			46.3	66
30.9			48	86			44.5	59
37.4			46	76			44.0	43
Series C								
14.4	5	.426	0	120	6	.645	21.2	110
23.7			4.3	106			41.0	89
30.9			18.7	94			42.2	72
37.4			27.5	84			47.3	59
14.4	7	.809	48.6	103	8	.413	29.3	94
23.7			52.9	76			36.3	89
30.9			52.1	56			37.4	78
37.4			53.2	38			41.4	69

TABLE III CON'T

Series C con't

L/D	RUN	$q/A \times 10^{-6}$ Btu/hr ft^2	ΔT_{sat} ^oF	ΔT_{sub} ^oF	RUN	$q/A \times 10^{-6}$ Btu/hr ft^2	ΔT_{sat} ^oF	ΔT_{sub} ^oF
14.4	9	.626	43	91	10	.855	55.2	82
23.7			44.6	71			57.7	54
30.9			47.6	55			53.1	47
37.4			50.2	41			53.4	26
14.4	11	.979	58.3	80				
23.7			59.5	48				
30.9			53.6	21				
37.4			56.1	0				
Series D								
14.4	3	.445	35	87	4	.52	45.5	79
23.7			42.7	72			50.4	62
30.9			45	60			52.7	48
37.4			50	49			57	37

TABLE III CON'T

Series D con't

L/D	RUN	q/A x 10^{-6} Btu/hr ft^2	ΔT_{sat} °F	ΔT_{sub} °F	RUN	q/A x 10^{-6} Btu/hr ft^2	ΔT_{sat} °F	ΔT_{sub} °F
14.4	5	.62	53.3	70	6	.735	56	70
23.7			56.0	50			57.9	45
30.9			52.4	34			53.9	27
37.4			53.2	20			56.7	9
14.4	7	.85	55.4	67	8	1.033	57.6	58
23.7			56.0	39			55.2	24
30.9			59.7	17			49.4	0
37.4			63.1	0			53	0
14.4	9	1.172	60	55				
23.7			58	16				
30.9			53	0				
37.4			57	0				

TABLE III CON'T

Series E

L/D	RUN	$q/A \times 10^{-6}$ Btu/hr ft^2	ΔT_{sat} ^oF	ΔT_{sub} ^oF	RUN	$q/A \times 10^{-6}$ Btu/hr ft^2	ΔT_{sat} ^oF	ΔT_{sub} ^oF
14.4	1	.306	19.4	65	2	.44	32.9	61
23.7			25.9	55			39.9	47
30.9			27.7	47			47.2	36
37.4			32.6	40			51.3	26
14.4	3	.542	40.9	51	4	.58	57.9	48
23.7			43.1	34			52.1	29
30.9			40.3	20			50.3	15
37.4			42.8	8			42.8	1
14.4	5	.72	55.5	50				
23.7			53.8	27				
30.9			48.3	9				
37.4			50.7	0				

TABLE III CON'T

Series G

L/D	RUN	$q/A \times 10^{-6}$ Btu/hr ft^2	ΔT_{sat} ^oF	ΔT_{sub} ^oF	RUN	$q/A \times 10^{-6}$ Btu/hr ft^2	ΔT_{sat} ^oF	ΔT_{sub} ^oF
14.4	5	.841	16.3	210	6	1.0	35.4	202
23.7			21.9	195			40.6	184
30.9			28.8	185			42.7	172
37.4			28.1	174			39.2	166
14.4	7	1.17	54.1	194	8	.785	7.2	201
23.7			61.0	175			22.3	188
30.9			60.5	160			27.0	178
37.4			50.8	147			27.1	169
14.4	9	1.27	63.7	172	10	1.35	68.2	167
23.7			67.8	150			73.0	144
30.9			65.5	134			68.7	127
37.4			55.5	120			57.2	112

TABLE III CON'T

Series G con't

L/D	RUN	$q/A \times 10^{-6}$ Btu/hr ft^2	ΔT_{sat} ^oF	ΔT_{sub} ^oF	RUN	$q/A \times 10^{-6}$ Btu/hr ft^2	ΔT_{sat} ^oF	ΔT_{sub} ^oF
14.4	11	1.44	72.1	162				
23.7			76.6	137				
30.9			72.1	117				
37.4			60.7	102				
Series H								
14.4	5	.65		134	6	.554		124
23.7			13.2	114			5.3	114
30.9			25.5	105			15.2	107
37.4			28.8	98			17.8	100
14.4	7	.71	25	121	8	.772	35.8	119
23.7			34.5	109			43.4	107
30.9			39.4	100			41.0	97
37.4			40.6	92			41.1	89

TABLE III CON'T

Series H con't

L/D	RUN	q/A x 10^{-6} Btu/hr ft^2	ΔT_{sat} °F	ΔT_{sub} °F	RUN	q/A x 10^{-6} Btu/hr ft^2	ΔT_{sat} °F	ΔT_{sub} °F
14.4	9	.83	45.8	116	10	.913	53.7	117
23.7			49.8	103			58.4	102
30.9			51.1	93			57.9	90
37.4			47.8	83			52.4	80
14.4	11	1.01	60.9	114				
23.7			66.7	97				
30.9			65.0	84				
37.4			54.5	72				
Series I								
14.4	2	.236	9.1	211	3	.264	15.3	208
23.7			14.3	196			25.8	192
30.9			12.2	184			24.4	176
37.4			14.4	173			23.2	164

TABLE III CON'T

Series I con't

L/D	RUN	q/A x 10^{-6} Btu/hr ft^2	ΔT_{sat} ^oF	ΔT_{sub} ^oF	RUN	q/A x 10^{-6} Btu/hr ft^2	ΔT_{sat} ^oF	ΔT_{sub} ^oF
14.4	4	.291	19.2	204	5	.339	32.1	197
23.7			28.8	185			32.7	175
30.9			28.1	170			32.2	157
37.4			28.1	156			29.9	142
14.4	6	.404	44.3	190	7	.475	49.2	181
23.7			47.6	164			54.4	150
30.9			38.1	142			50.2	127
37.4			38.1	126			39.3	105
Series J								
14.4	1	.159		114	2	.216	26.8	111
23.7				104			35.7	97
30.9			8.3	96			33.1	86
37.4			11.6	88			34.9	76

TABLE III CON'T

Series J con't

L/D	RUN	$q/A \times 10^{-6}$ Btu/hr ft^2	ΔT_{sat} °F	ΔT_{sub} °F	RUN	$q/A \times 10^{-6}$ Btu/hr ft^2	ΔT_{sat} °F	ΔT_{sub} °F
14.4	3	.297	43.2	101	4	.348	45.7	93
23.7			50.0	80			51.8	79
30.9			46.9	65			48.8	51
37.4			41.2	52			42.5	34
14.4	5	.407	44.6	89	6	.48	56.3	81
23.7			59.2	63			58.6	50
30.9			56.3	42			52.6	25
37.4			46.2	24			44.7	4
14.4	7	.529	58.9	72				
23.7			60.7	38				
30.9			62.9	10				
37.4			45.7	0				

TABLE IV

BULK BOILING DATA

Series E

L/D	RUN	$q/A \times 10^{-6}$ Btu/hr ft^2	ΔT_{sat} ^oF	ΔT_{sub} ^oF	$h \times 10^{-3}$ Btu/hr ft^2 ^oF	x^*	T_b ^oF	$1/X_{TT}$	h/h_L
14.4	6	.839	62.9	108	7.26				
23.7			64.3	82.3	10.7				
30.9			55.0	55.0	15.3	.004	295.8	.1	5.02
37.4			47.6	47.6	17.6	.028	294.4	.7	5.81
14.4	7	.958	64.3	89.3	10.72		275		
23.7			65.9	65.9	14.55		299.2		
30.9			57.3	57.3	16.72	.02	297.9	.45	5.49
37.4			50.7	50.7	18.9	.046	295.3	1.13	6.23
14.4	8	1.14	67.8	94.5	12.1		275		
23.7			68.5	68.5	16.8	.004	301.5	0.1	5.47
30.9			59.9	59.9	19.1	.056	299.8	1.3	6.23
37.4			52.3	52.3	21.8	.077	296.5	1.82	7.16

* x denotes quality, i.e., fraction of steam by weight.

TABLE IV CON'T

Series E con't

L/D	RUN	$q/A \times 10^{-6}$ Btu/hr ft^2	ΔT_{sat} ^oF	ΔT_{sub} ^oF	$h \times 10^{-3}$ Btu/hr ft^2 ^oF	x	T_b ^oF	$1/X_{TT}$	h/h_L
14.4	9	1.416	69.7	85.2	16.6		293		
23.7			70.4	70.4	20.1	.056	306.8	1.2	6.5
30.9			61.6	61.6	23.0	.095	304.7	2.1	7.45
37.4			56.0	56.0	25.3	.137	299	3.16	8.29
14.4	10	1.572	65.3	69.3	22.7		306.2		
23.7			73.0	73.0	21.56	.055	308	1.2	6.95
30.9			68.3	68.3	23.0	.102	304.7	2.25	7.45
37.4			61.0	61.0	25.8	.149	298.7	3.4	8.45
14.4	11	1.68	66.9	72.0	23.4				
23.7			78.6	78.6	21.4	.057	309.4	1.2	6.89
30.9			74.5	74.5	22.6	.107	306.5	2.35	7.31
37.4			66	66	25.5	.156	300	3.5	8.32

TABLE IV CON'T

Series F

L/D	RUN	q/A x 10^{-6} Btu/hr ft^2	ΔT_{sat} ^oF	ΔT_{sub} ^oF	h x 10^{-3} Btu/hr ft^2 ^oF	x	T_b ^oF	$1/X_{TT}$	h/h_L
14.4	1	.396	54.2	71.0	5.58		277.7		
23.7			59.5	63.3	6.25		290.3		
30.9			50.4	50.4	7.84	.007	293.7	0.2	2.59
37.4			45.4	45.4	8.73	.017	293	0.4	2.88
14.4	2	.477	57.9	70.7	6.75		282.9		
23.7			62.3	62.3	7.66	.0043	295.3	0.1	2.53
30.9			50.5	50.5	9.45	.0183	294.5	0.45	3.11
37.4			47.2	47.2	10.1	.0317	293.3	0.8	3.34
14.4	3	.581	62.4	62.4	9.32	.00-	297.6		
23.7			62.6	62.6	9.28	.023	296.5	0.55	3.05
30.9			51.9	51.9	11.2	.0416	295.3	1.0	3.70
37.4			48.2	48.2	12.04	.0587	294	1.42	3.98

TABLE IV CON'T

Series F

L/D	RUN	q/A x 10^{-6} Btu/hr ft^2	ΔT_{sat} ^oF	ΔT_{sub} ^oF	h x 10^{-3} Btu/hr ft^2 ^oF	x	T_b ^oF	$1/X_{TT}$	h/h_L
14.4	4	.701	62.3	62.3	11.1	.0115	299.6	0.24	3.63
23.7			62.5	62.5	11.21	.0472	297.0	1.15	3.68
30.9			52.1	52.1	13.46	.0632	296.3	1.55	4.42
37.4			48.7	48.7	14.4	.0844	293.8	2.05	4.75
14.4	5	.773	62.1	62.1	12.44	.0078	301.2	0.2	4.05
23.7			61.1	61.1	12.65	.0359	299.7	0.87	4.14
30.9			51.0	51.0	15.16	.0598	297.7	1.43	4.97
37.4			47.4	47.4	16.3	.0825	294.2	2.0	5.38
14.4	6	.868	67	67	12.94	.0132	302	0.35	4.22
23.7			63.8	63.8	13.6	.0454	300.9	1.04	4.44
30.9			55.3	55.3	15.7	.0725	298.2	1.7	5.15
37.4			50.6	50.6	17.14	.0975	294.6	2.35	5.65

TABLE IV CON'T

Series F con't

L/D	RUN	$q/A \times 10^{-6}$ Btu/hr ft^2	$\Delta T_{sat} = \Delta T_{sub}$ °F	$h \times 10^{-3}$ Btu/hr ft^2 °F	x	T_b °F	$1/X_{TT}$	h/h_L
14.4	7	1.06	69.8	15.2	.03	307.4	0.62	4.91
23.7			67.0	15.8	.069	304.8	1.5	5.14
30.9			60.6	17.5	.102	501.3	2.3	5.7
37.4			55.7	19.1	.133	295.6	3.15	6.28
14.4	8	1.19	69.7	17.1	.0436	311.4	1.0	5.5
23.7			65.3	18.2	.0777	309.5	1.8	5.87
30.9			59.7	19.9	.1149	306.3	2.52	6.45
37.4			55.4	21.5	.159	299	3.46	7.05
14.4	9	1.37	70.1	19.55	.0476	315.0	1.05	6.26
23.7			67.8	20.2	.1005	311.7	2.25	6.5
30.9			65.2	21.0	.145	306	3.39	6.8
37.4			58.2	23.55	.1843	300.3	4.14	7.68

TABLE IV CON'T

Series F con't

L/D	RUN	$q/A \times 10^{-6}$ Btu/hr ft^2	$\Delta T_{sat} + \Delta T_{sub}$ °F	$h \times 10^{-3}$ Btu/hr ft^2 °F	x	T_b °F	$1/X_{TT}$	h/h_L
14.4	10	1.453	66.8	21.8	.064	319.9	1.22	6.96
23.7			65.2	22.3	.121	319.9	2.46	7.14
30.9			62.7	23.2	.168	310.2	3.65	7.46
37.4			54.4	26.75	.212	302.5	4.70	8.68
14.4	11	1.61	81.3	19.8	.0668	322.7	1.25	6.3
23.7			80.8	19.94	.129	318.5	2.55	6.37
30.9			75.0	21.45	.191	313.8	3.92	6.9
37.4			67.1	24.0	.227	305.9	4.98	7.77
14.4	12	1.79	73.1	24.53	.0848	330.3	1.57	7.77
23.7			71.2	25.2	.141	328.7	2.66	8.00
30.9			66.3	27.1	.196	325	3.77	8.60
37.4			59.0	30.4	.233	314	4.85	9.86

TABLE IV CON'T

Series K

L/D	RUN	q/A x 10^{-6} Btu/hr ft^2	$\Delta T_{sat} = \Delta T_{sub}$ °F	h x 10^{-3} Btu/hr ft^2 °F	x	T_b °F	$1/X_{TT}$	h/h_L
14.4	1	.202	41.7	4.84	.0055	294.2	0.1	2.8
23.7			42.6	4.75	.0214	293.9	0.5	2.75
30.9			40.9	4.94	.0319	293.6	0.75	2.85
37.4			36.6	5.52	.0421	293.5	1.0	3.2
14.4	2	.271	48.4	5.6	.0172	293.8	0.38	3.24
23.7			46.9	5.78	.0372	293.4	0.87	3.35
30.9			45.2	6.00	.0526	293.1	1.25	3.48
37.4			37.2	7.29	.0665	292.7	1.6	4.23
14.4	3	.345	53.5	6.45	.0197	294.9	0.46	3.73
23.7			51.8	6.66	.0452	294.5	1.06	3.86
30.9			45.0	7.66	.065	294	1.54	4.44
37.4			45.9	8.44	.083	293.4	1.97	4.89

TABLE IV CON'T

Series K con't

L/D	RUN	$q/A \times 10^{-6}$ Btu/hr ft^2	$\Delta T_{sat} = \Delta T_{sub}$ ^oF	$h \times 10^{-6}$ Btu/hr ft^2 ^oF	x	T_b ^oF	$1/X_{TT}$	h/h_L
14.4	4	.42	55.8	7.53	.0307	294.6	0.72	4.36
23.7			54.3	7.74	.0619	293.8	1.46	4.48
30.9			47.9	8.77	.0864	293	2.04	5.09
37.4			43.2	9.72	.1082	292.4	2.57	5.65
14.4	5	.514	55.8	7.81	.044	296.4	1.02	4.5
23.7			63.7	8.07	.082	295.5	1.91	4.66
30.9			58.8	8.75	.112	294.4	2.65	5.065
37.4			53.9	9.54	.138	293.4	3.49	5.53
14.4	6	.625	62.3	10.03	.058	296.3	1.354	5.79
23.7			62.0	10.09	.1039	295.1	2.43	5.835
30.9			55.2	11.32	.140	294	3.35	6.56
37.4			49.4	12.67	.162	292.7	3.7	7.35

TABLE IV CON'T

Series L

L/D	RUN	$q/A \times 10^{-6}$ Btu/hr ft^2	$\Delta T_{sat} = \Delta T_{sub}$ °F	$h \times 10^{-3}$ Btu/hr ft^2 °F	x	T_b °F	$1/X_{TT}$	h/h_L
57.9	1	.319	34.9	9.13	.048	297.1	1.1	3.0
64.1			31.0	10.33	.0569	294.8	1.34	3.41
72.4			30.3	10.52	.0697	293.5	1.66	3.48
78.5			31.2	10.21	.0793	291.4	1.95	3.40
57.9	2	.419	36.3	11.52	.0791	302	1.75	3.755
64.1			33.8	12.38	.0912	300	2.04	4.04
72.4			33.5	12.49	.1076	297	2.46	4.1
78.5			35.3	11.85	.1206	294.5	2.85	3.91
57.9	3	.525	41.5	12.65	.0935	304.5	2.03	4.1
64.1			39.2	13.4	.1088	307.1	2.4	4.36
72.4			38.9	13.5	.129	298.4	2.94	4.43
78.5			39.7	13.22	.145	295.2	3.4	4.36

TABLE IV CON'T

Series L con't

L/D	RUN	$q/A \times 10^{-6}$ Btu/hr ft^2	ΔT_{sat}	= ΔT_{sub} °F	$h \times 10^{-3}$ Btu/hr ft^2 °F	x	T_b °F	$1/X_{TT}$	h/h_L
57.9	4	.655		47.4	13.72	.1188	308.4	2.54	4.43
64.1				44.5	14.72	.1372	305.0	2.98	4.775
72.4				43.9	14.91	.1731	300	3.86	4.88
78.5				44.9	14.63	.1835	295.6	4.3	4.82
57.9	5	.725		50.6	14.3	.1276	310.7	2.68	4.6
64.1				46.7	15.5	.1596	307.0	3.42	5.01
72.4				45.7	15.84	.1878	301.1	4.15	5.27
78.5				46.4	15.61	.210	295.9	4.95	5.14
57.9	6	.878		55.5	15.81	.157	317.3	3.16	5.055
64.1				52.3	16.8	.1829	312.9	3.8	5.4
72.4				50.4	17.42	.217	307	4.69	5.64
78.5				52.1	16.83	.243	302	5.4	5.49

TABLE IV CON'T

Series M

L/D	RUN	$q/A \times 10^{-6}$ Btu/hr ft^2	$\Delta T_{sat} = \Delta T_{sub}$ ^oF	$h \times 10^{-3}$ Btu/hr ft^2 ^oF	x	T_b ^oF	$1/X_{TT}$	h/h_L
57.9	1	.202	31.7	6.35	.087	295.4	2.02	3.67
64.1			29.2	6.74	.0975	294.6	2.59	3.9
72.4			29.3	6.87	.1112	293.6	2.63	3.98
78.5			29.8	6.75	.122	292.7	2.9	3.92
57.9	2	.354	36.9	9.56	.1419	297.9	3.25	5.5
64.1			34.4	10.26	.171	296.7	3.99	5.92
72.4			34.4	10.26	.1955	295	4.6	5.94
78.5			35.2	10.02	.213	293.5	5.1	5.82
57.9	3	.468	42.4	11.03	.203	300	4.6	6.32
64.1			39.1	11.94	.2306	298.4	5.45	6.88
72.4			38.9	12.01	.260	296	6.4	6.94
78.5			38.9	12.01	.283	293.9	7.1	6.95

TABLE IV CON'T

L/D	RUN	$q/A \times 10^{-6}$ Btu/hr ft^2	$\Delta T_{sat} = \Delta T_{sub}$ ^oF	$h \times 10^{-3}$ Btu/hr ft^2 ^oF	x	T_b ^oF	$1/X_{TT}$	h/h_L
Series M con't								
57.9	4	.564	50.3	11.2	.238	301.4	5.9	6.4
64.1			44.1	12.79	.2665	299.3	6.3	7.44
72.4			42.9	13.13	.306	296.2	7.7	7.59
78.5			43.8	12.87	.334	293.7	9.1	7.47
57.9	5	.704	52.2	13.48	.3005	304.2	7.1	7.68
64.1			48.1	14.61	.3372	301.7	8.3	8.35
72.4			47.8	14.71	.3852	296.7	10.4	8.49
78.5			47.5	14.8	.422	294.2	12.0	8.58
Series N								
30.9	1	.517	52.4	9.87	.0318	307.9	0.61	3.15
37.4			37.9	13.63	.0436	307	0.9	4.36
72.4			37.2	13.9	.1234	299.7	2.76	4.54
78.5			35.0	14.76	.139	296.5	3.22	4.85

TABLE IV CON'T

Series N con't

L/D	RUN	$q/A \times 10^{-6}$ Btu/hr ft^2	$\Delta T_{sat} = \Delta T_{sub}$ ^oF	$h \times 10^{-3}$ Btu/hr ft^2 ^oF	x	T_b ^oF	$1/X_{TT}$	h/h_L
30.9	2	.711	57.4	12.4	.0501	319.5	0.98	3.96
37.4			52.4	13.59	.0695	318.4	1.33	4.34
72.4			49.2	14.45	.1813	303.8	3.94	4.69
78.5			45.9	15.5	.203	299.3	4.5	5.06
30.9	3	.866	62.0	13.98	.0625	325.7	1.2	4.44
37.4			57.1	15.18	.0858	324.5	1.53	4.82
72.4			55.8	15.53	.222	307.5	4.88	5.02
78.5			51.4	16.87	.248	302.1	5.55	5.49
30.9	4	1.005	61.4	16.4	.0745	332.2	1.35	5.19
37.4			55.7	17.73	.102	331.0	1.85	5.62
72.4			55.7	17.73	.2585	312.8	2.74	5.7
78.5			50.9	19.8	.288	307.1	3.28	6.4

TABLE IV CON'T

Series N con't

L/D	RUN	$q/A \times 10^{-6}$ Btu/hr ft^2	$\Delta T_{sat} = \Delta T_{sub}$ ^oF	$h \times 10^{-3}$ Btu/hr Ft^2 ^oF	x	T_b ^oF	$1/X_{TT}$	h/h_L
30.9	5	1.169	35.8	32.6	.0885	335.4	1.58	10.3
37.4			30.3	38.6	.177	334.3	3.21	12.2
72.4			31.7	36.85	.30	314.5	6.5	11.8
78.5			26.0	45.0	.332	309.6	7.8	14.5

TABLE V

RANGE OF VARIABLES

T.S.	Series	T_i °F	G x 10^{-6} $lb_m/hr\ ft^2$	q/A x 10^{-6} Btu/hr ft^2	
1	A	43-57	1.19	.043-.954	a,b*
1	B	149-153	1.19	.092-.918	a,b
2	C	150-168	1.19	.125-.979	a,b
2	D	184-187	1.19	.085-1.33	a,b
2	E	212-228	1.19	.306-1.68	b,c
2	F	249-289	1.19	.477-1.79	c
2	G	54-95	2.38	.319-1.35	a,b
2	H	152-156	2.38	.22 -1.007	a,b
2	I	55-63	.59	.236-.475	a,b
2	J	158-166	.59	.159-.5285	b
2	K	271-285	.59	.202-.625	c
3	L	276-293	1.19	.3185-.878	c
3	M	285-291	.59	.2016-.704	c
3 mod.	N	281-290	1.19	.5165-1.169	c

* denotes types of data obtained

a - non-boiling

b - subcooled nucleate boiling

c - bulk boiling

BIBLIOGRAPHY

(1) Bergles, A.E. and Rohsenow, W.M. "Forced Convection Surface-Boiling Heat Transfer and Burnout in Tubes of Small Diameter," DSR Project Report No. 8767-21, Mech. Eng. Dept., M.I.T., May, 1962.

(2) Maulbetsch, J.S. "A Study of System-Induced Instabilities in Forced Convection Flows with Subcooled Boiling," ScD. Thesis Mech. Eng. Dept., M.I.T., May, 1965

(3) Wessel, H.L. "Investigation of Forced-Convection Subcooled Boiling," S.B. Thesis, Mech. Eng. Dept., M.I.T., May 1964.

(4) McAdams, W.H. "Heat Transmission," Second Edition, McGraw-Hill, 1942.

(5) Bergles, A.E. and Rohsenow, W.M. "Determination of Forced-Convection Surface-Boiling Heat Transfer," Trans. ASME Journal of Heat Transfer, August, 1964

(6) Lowdermilk, W.H., Lanzo, C.D. and Siegel, B.L. "Investigation of Boiling Burnout and Flow Stability for Water Flowing in Tubes," NACA-TN 4382, September, 1958.

(7) Loosmore, C.S. and Skinner, B.C. "Subcooled Critical Heat Flux for Water in Round Tubes," S.M. Thesis, Mech. Eng. Dept., M.I.T. May, 1965.

(8) Lopina, R.F. "Two Phase Critical Heat Flux to Low Pressure Water Flowing in Small Diameter Tubes," S.M. Thesis, Mech. Eng. Dept., M.I.T. May, 1965

(9) Waters, E.D., Anderson, J.K., Thorne, W.L., and Batch, J.M. "Experimental Observations of Upstream Burnout," AIChE Preprint 7 for SIXTH National Heat Transfer Conference, August, 1963.

(10) Seider, E.N. and Tate, G.E. "Heat Transfer and Pressure Drop in Liquids in Tubes," Ind. Eng. Chem., Vol. 28, 1936, pg.1424-1436.

(11) Bennett, J.A.R., Collier, J.G., Pratt, H.R.C., and Thornton, J.D. "Heat Transfer to Two-Phase Gas-Liquid Systems, Part I: Steam-Water Mixtures in the Liquid-Dispersed Region in an Annulus," Trans. Instn. Chem. Engrs., Vol. 39, 1961.

(12) Dengler, C.E. and Addoms, J.N. "Heat Transfer Mechanism for Vaporization of Water in a Vertical Tube," Chem. Eng. Prog. Symp. Series, Vol. 52, No. 18, 1956, pg. 95-103.

(13) Chen, J.C. "A Correlation for Boiling Heat Transfer to Saturated Fluids in Convective Flow," ASME paper No. 63-HT-34, May, 1963.

(14) Gouse, S.W. Jr. and Coumou, K.G. "Heat Transfer Inside a Horizontal Tube Evaporator," DSR Report No. 9649-1, Mech. Eng. Dept., M.I.T. June, 1964.

(15) Geidt, W.H. "Principles of Engineering Heat Transfer," D. Van Nostrand Co. Inc., 1957.

(16) Rohsenow, W.M. and Choi, H. "Heat, Mass, and Momentum Transfer," Prentice-Hall, 1961.

(17) Zuber, N. and Fried, E. "Two-Phase Flow and Boiling Heat Transfer to Cryogenic Liquids," ARS Journal, September, 1962.

(18) Levy, S. "Generalized Correlation of Boiling Heat Transfer," Trans. ASME Journal of Heat Transfer, February, 1959, pg. 37-42.

(19) Kutatelodze, S.S. "Boiling Heat Transfer," Int. Journal Heat and Mass Transfer, Vol. 4, 1961, pg. 31-45.

LIST OF FIGURES

Figure No.		Page
1	Schematic layout of experimental facility	74
2	Details of test section construction	75
3	Wall temperature correction chart for 5/16 inch stainless steel tube	76
4	The dependence of critical heat flux on exit quality	77
5	Correlation of forced-convection non-boiling data	78
6	Subcooled nucleate boiling curves	79
7	Wessel's fully-developed boiling data	80
8	Bulk boiling data T.S. 2	81
9	Bulk boiling data	82
10	Subcooled nucleate boiling with effect of L/D	82
11	Heat transfer coefficient vs quality T.S. 2. Mass velocity and heat flux as parameters	83
12	Comparison of heat transfer coefficient for T.S. 2 and 3. Heat flux as a parameter	84
13	Comparison of heat transfer coefficient for T.S. 2 and 3	85
14	Comparison of heat transfer coefficient for T.S. 2, 3, and 3 modified.	86
15	Correlation of heat transfer coefficient for T.S. 2, 3, and 3 modified.	87
16	Correlation of heat transfer coefficient for T.S. 2, and 3.	88

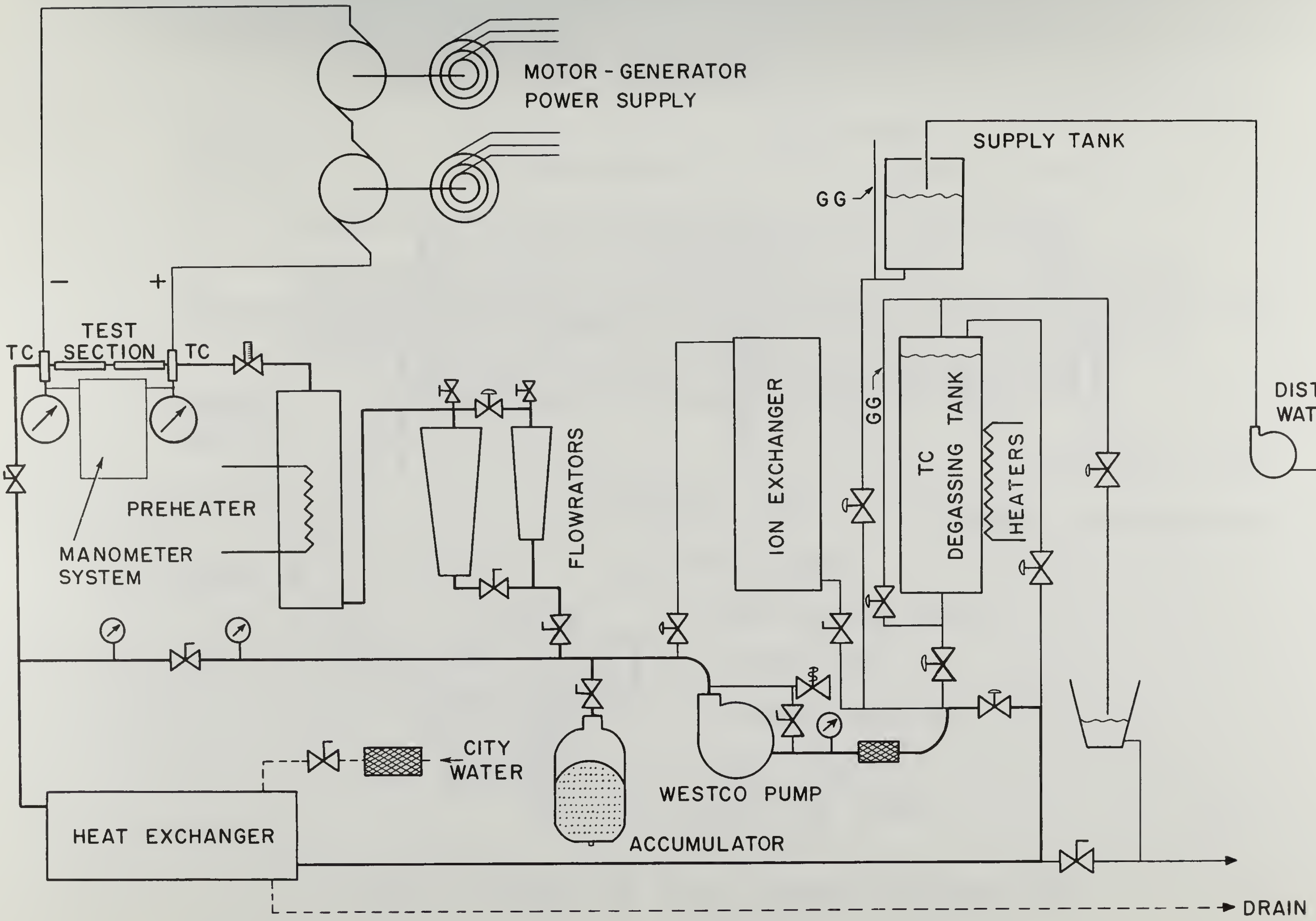

FIGURE 1

SCHEMATIC LAYOUT OF EXPERIMENTAL FACILITY

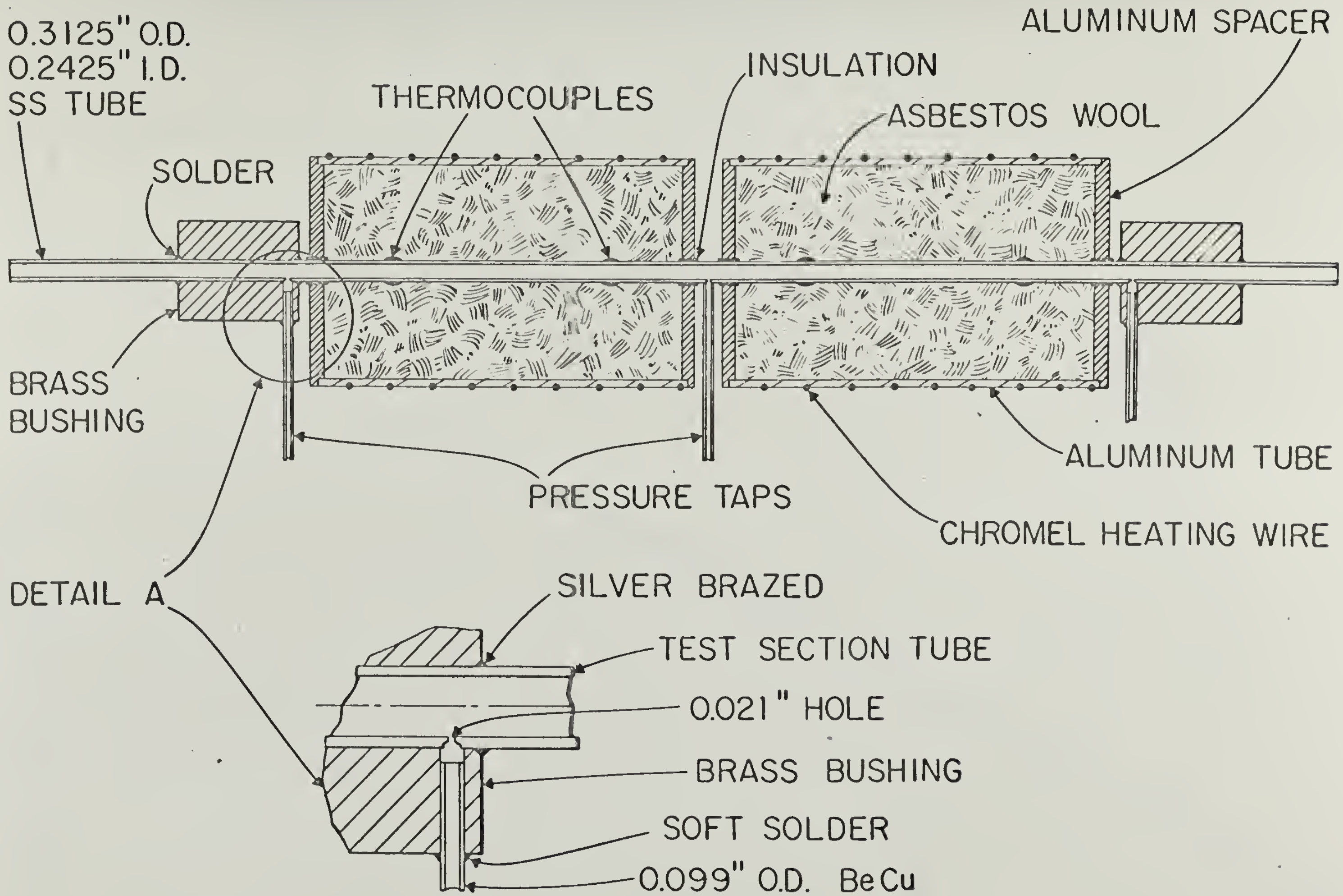

FIG. 2 DETAILS OF TEST SECTION CONSTRUCTION

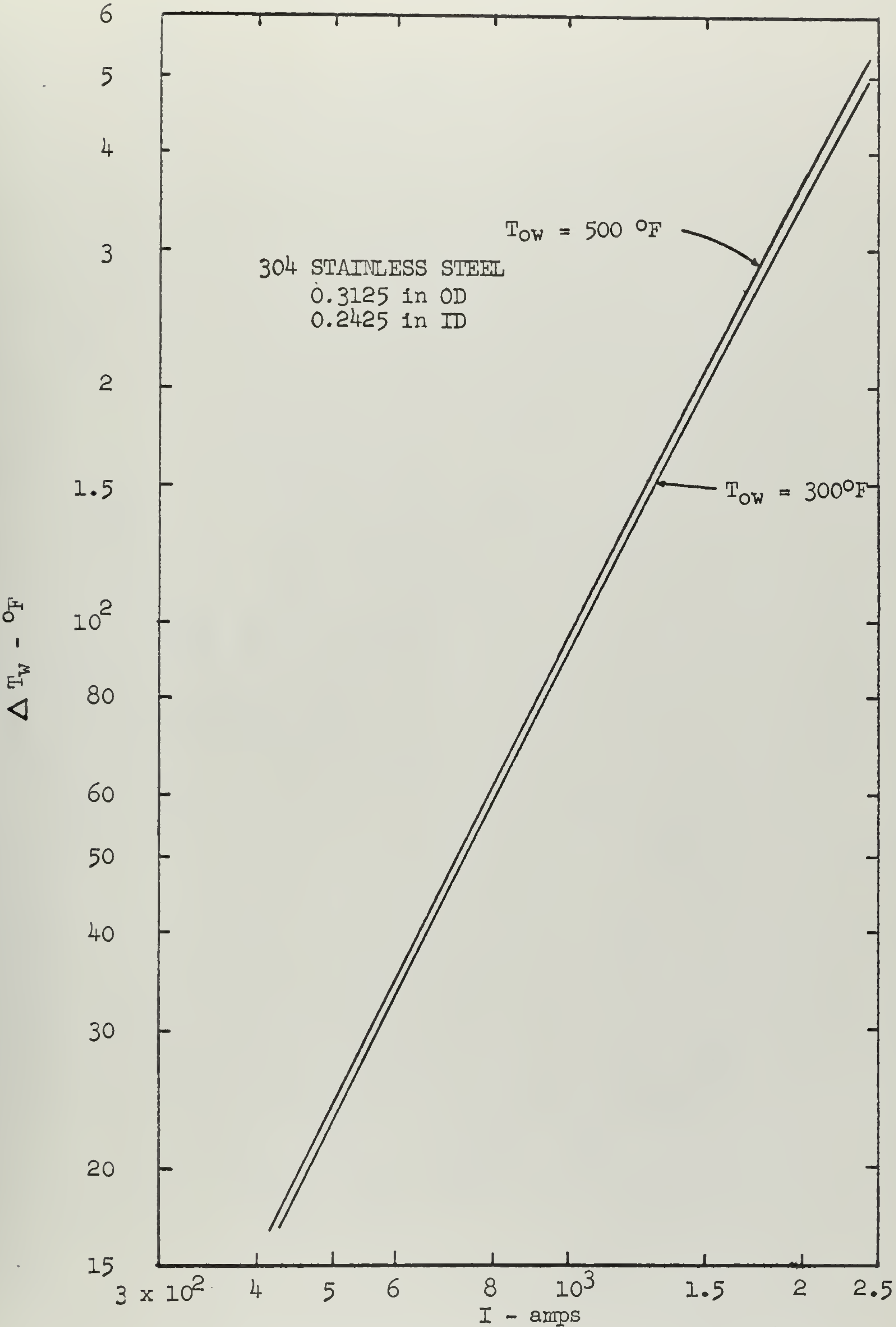

FIG. 3 WALL TEMPERATURE CORRECTION CHART FOR 5/16 INCH STAINLESS STEEL TUBE.

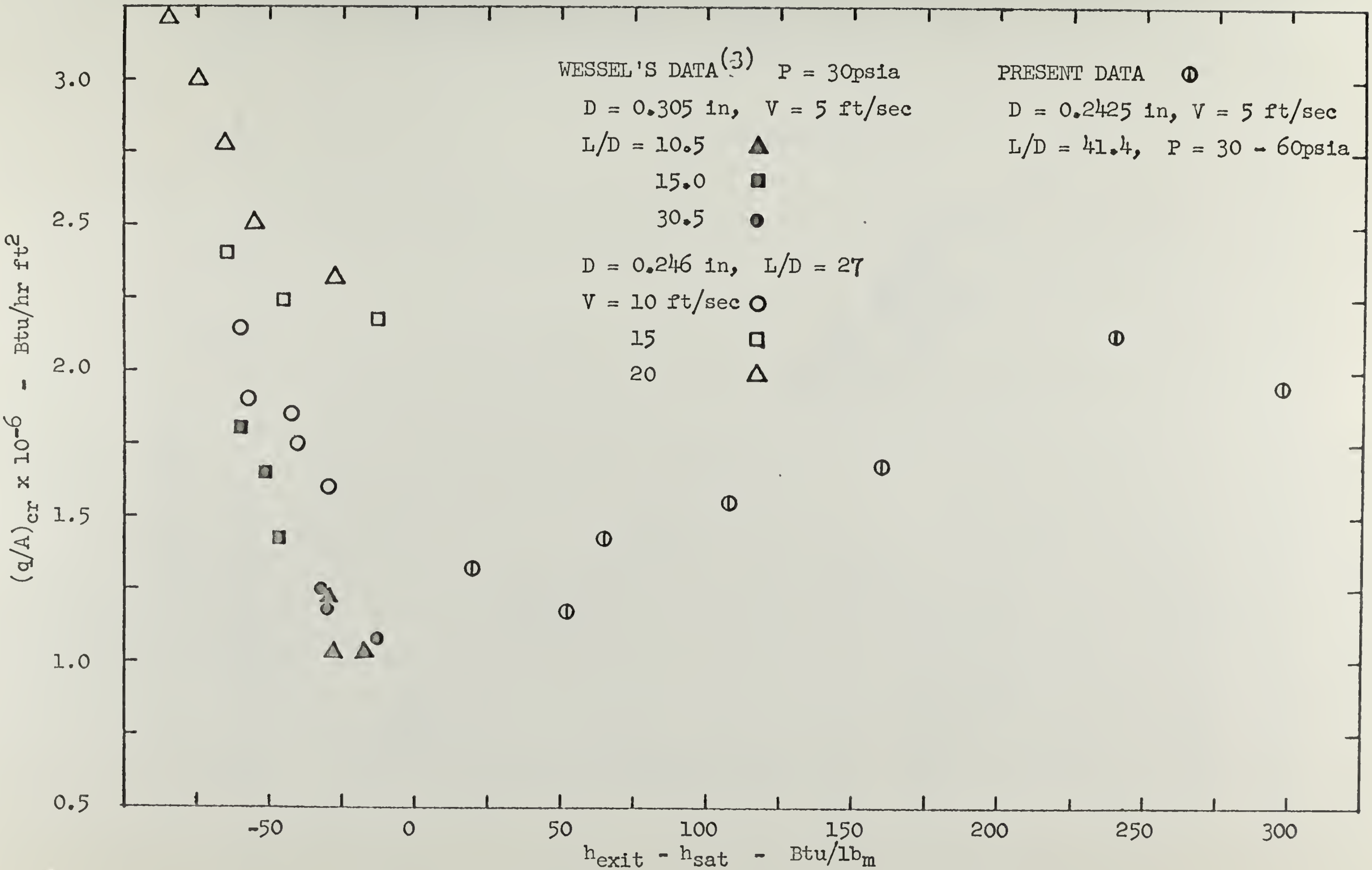

FIG. 4 THE DEPENDENCE OF CRITICAL HEAT ON EXIT QUALITY.

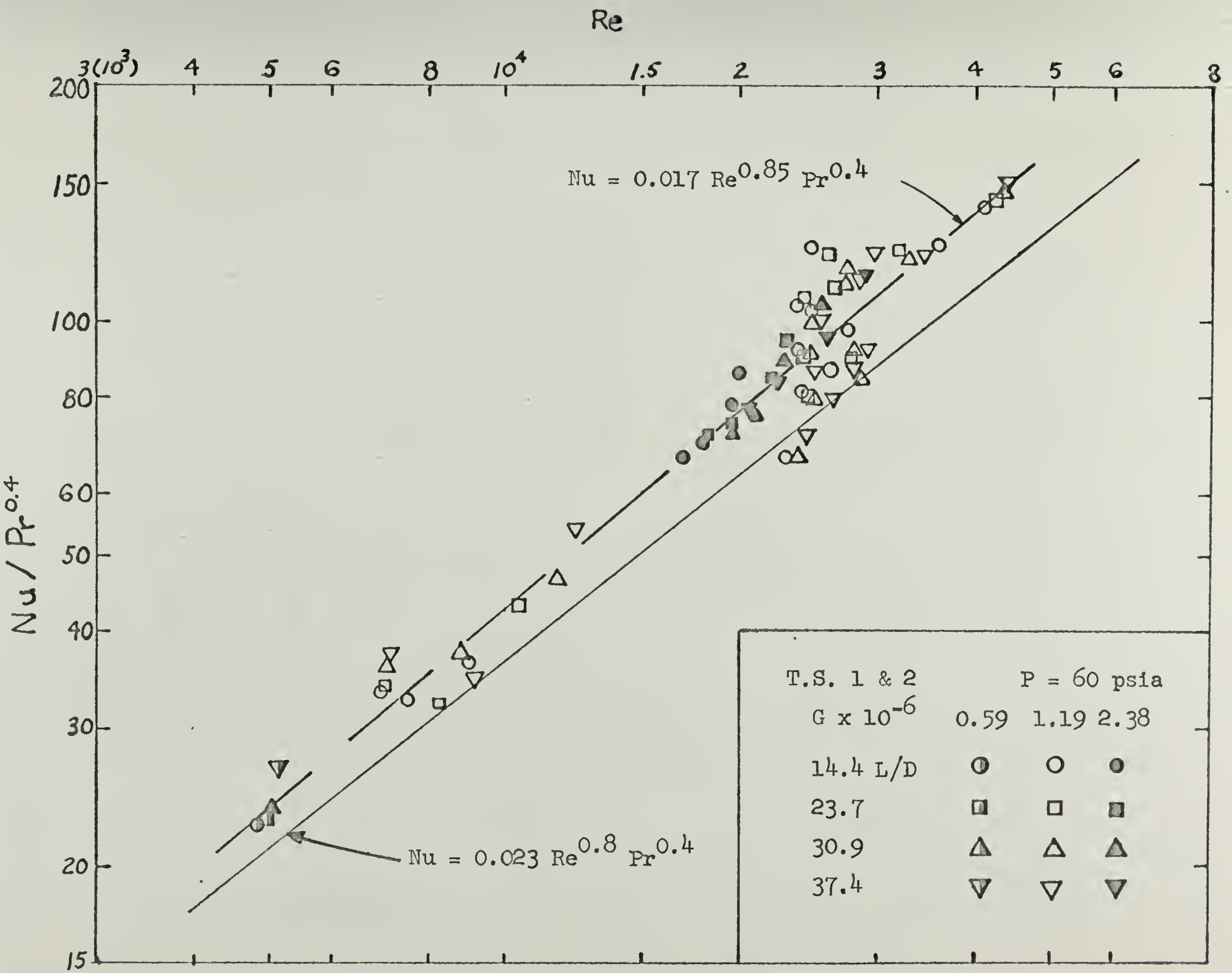

FIG. 5 CORRELATION OF FORCED-CONVECTION NON BOILING DATA.

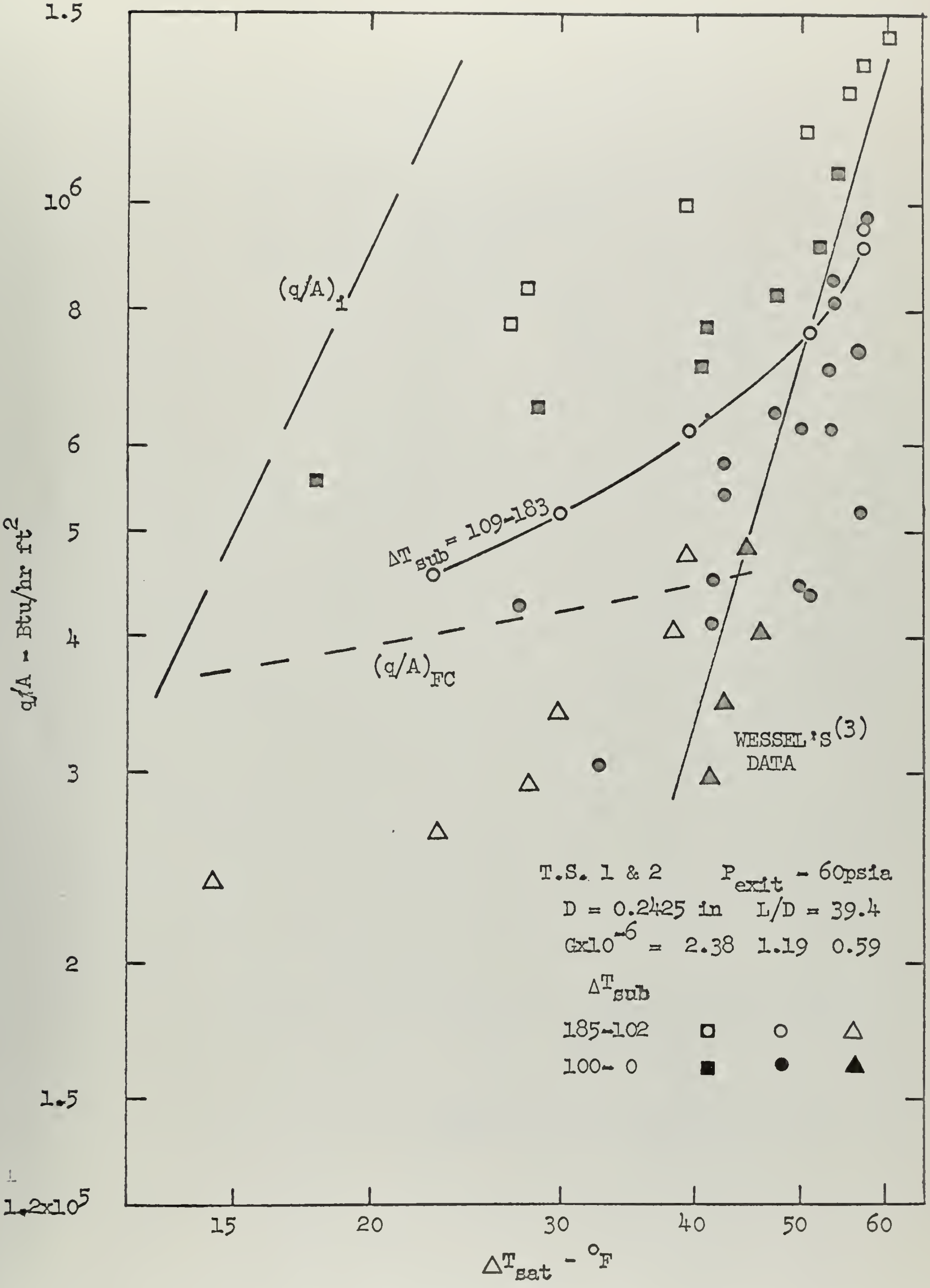

FIG. 6 SUBCOOLED NUCLEATE BOILING CURVES.

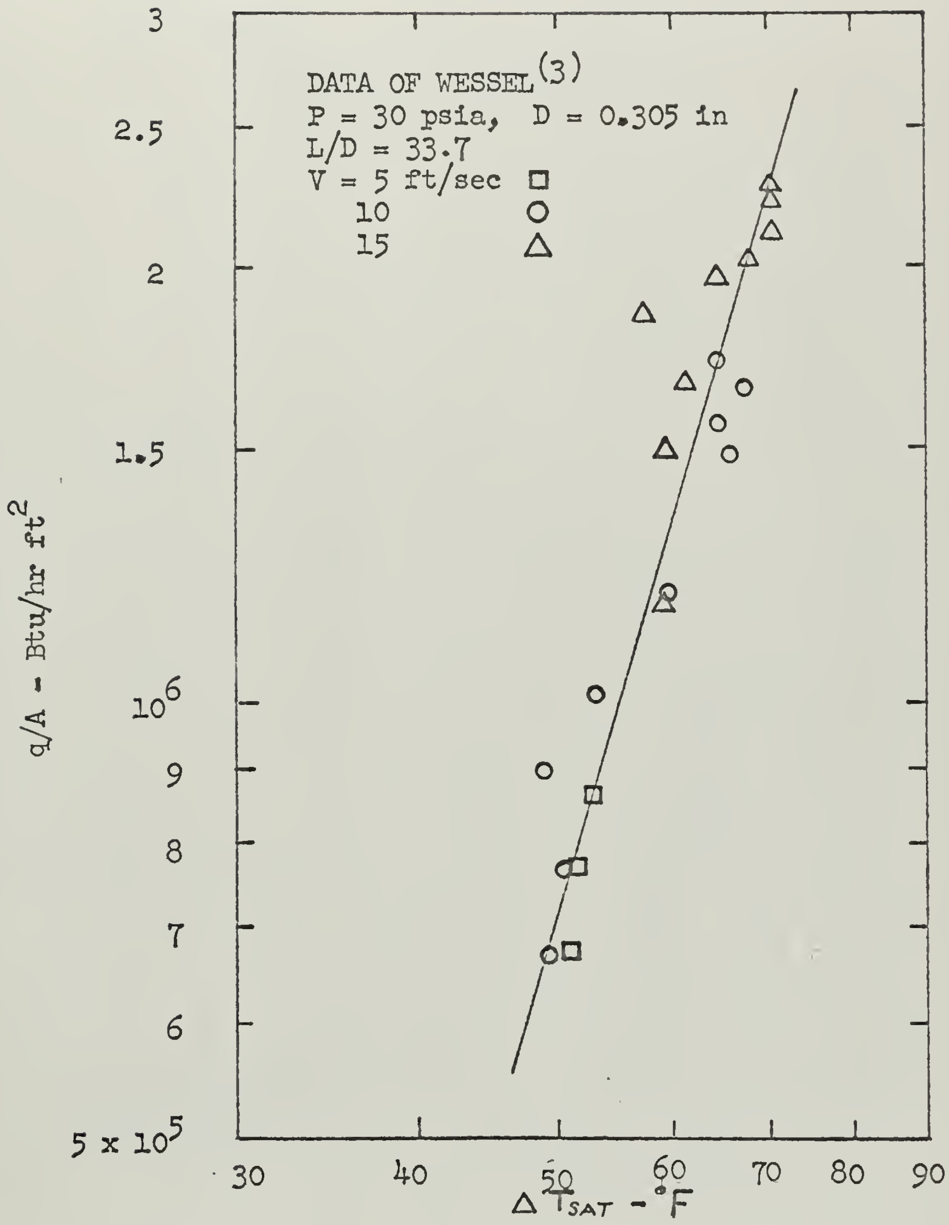

FIG. 7 WESSEL'S FULLY-DEVELOPED BOILING DATA.

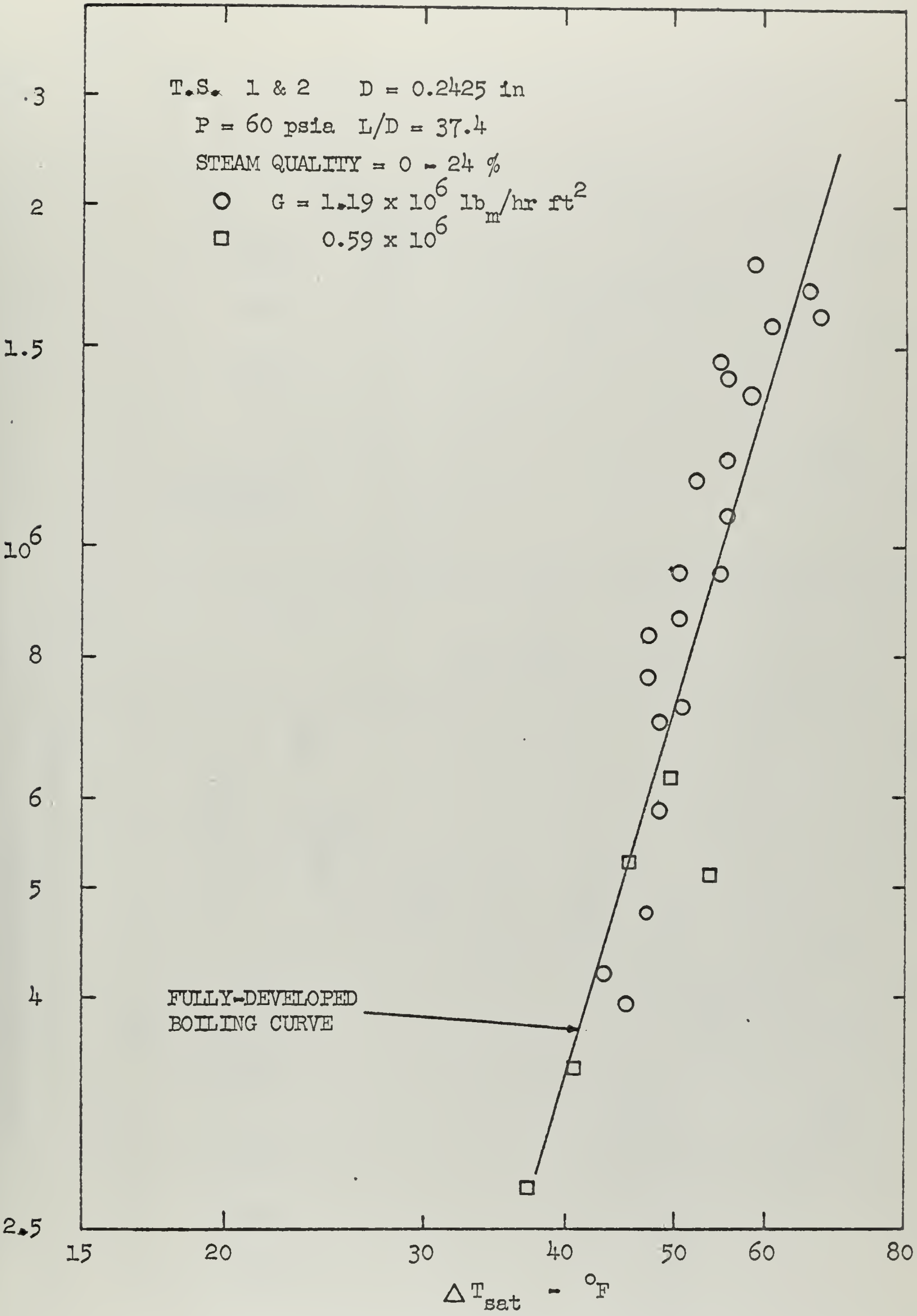

FIG. 8 BULK BOILING DATA T.S. 2

FIG.9 BULK BOILING DATA.

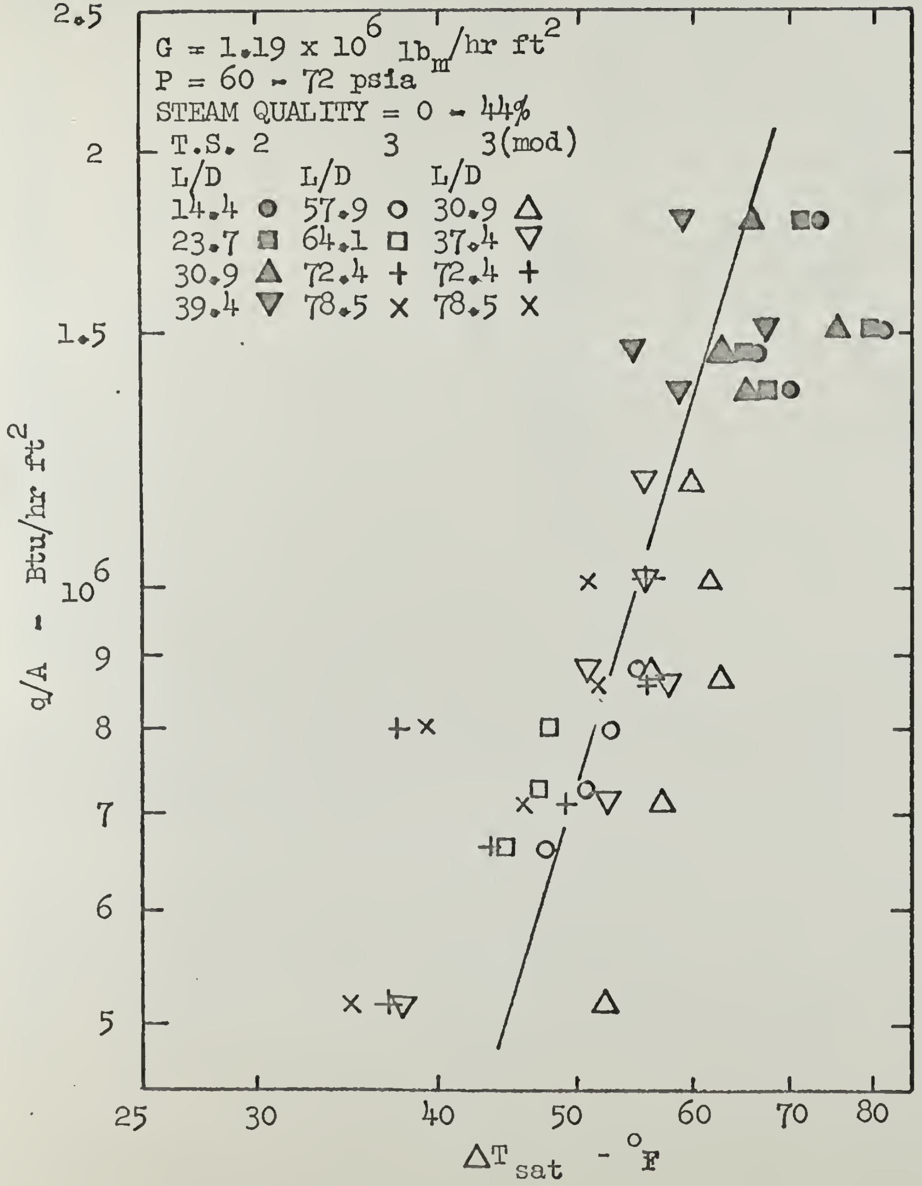

FIG. 10 SUBCOOLED NUCLEATE BOILING WITH EFFECT OF L/D.

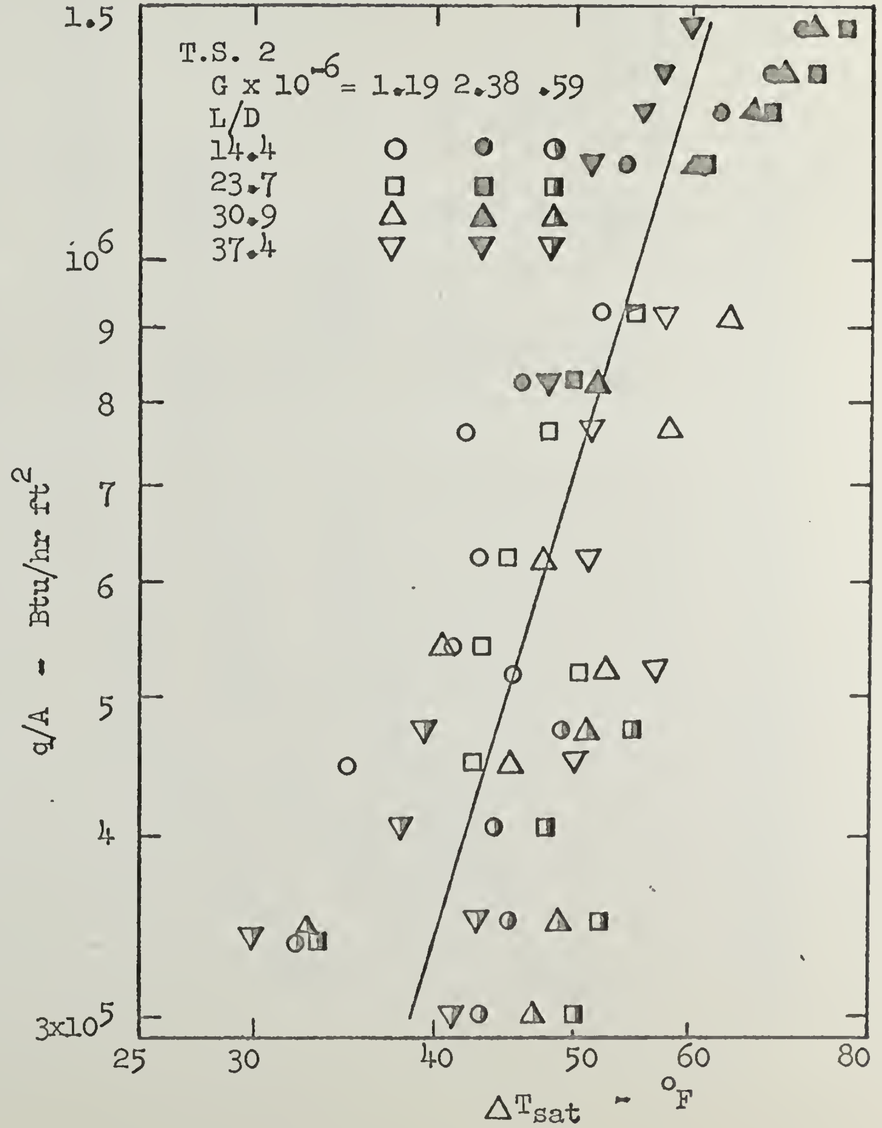

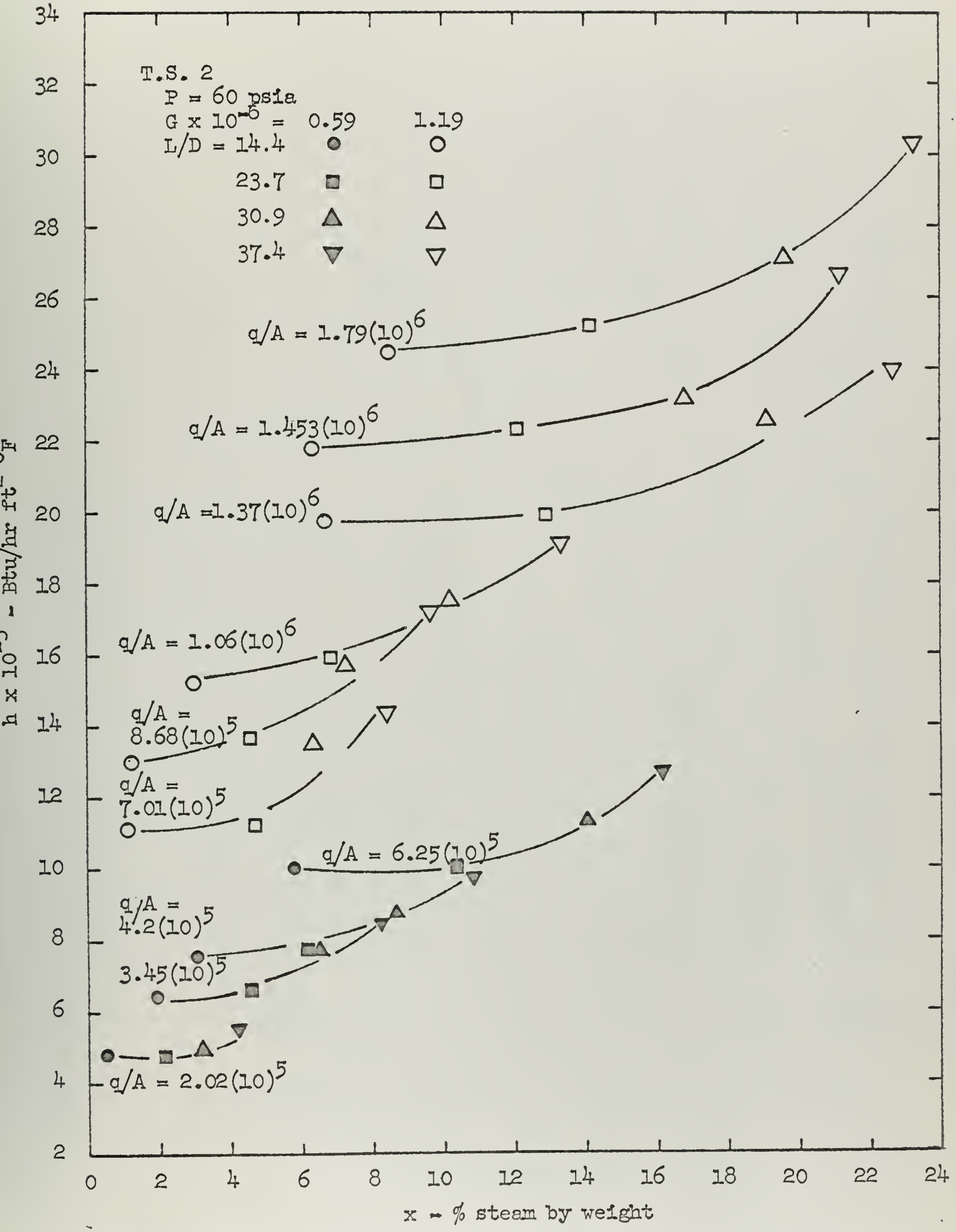

FIG. 11 HEAT TRANSFER COEFFICIENT VS QUALITY T.S. 2. MASS VELOCITY AND HEAT FLUX AS PARAMETERS.

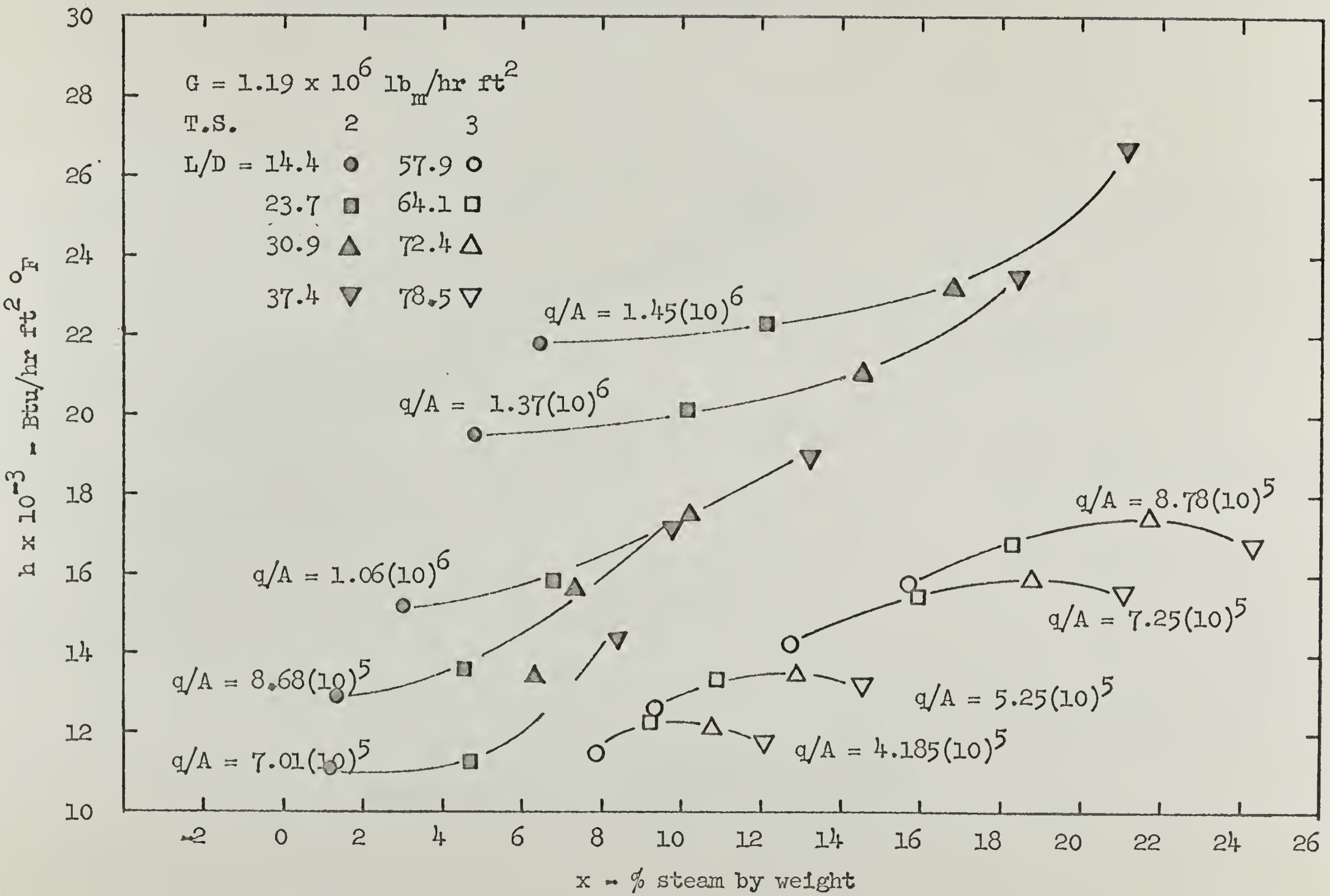

FIG. 12 COMPARISON OF HEAT TRANSFER COEFICIENT FOR T.S. 2 AND 3. HEAT FLUX AS A PARAMETER.

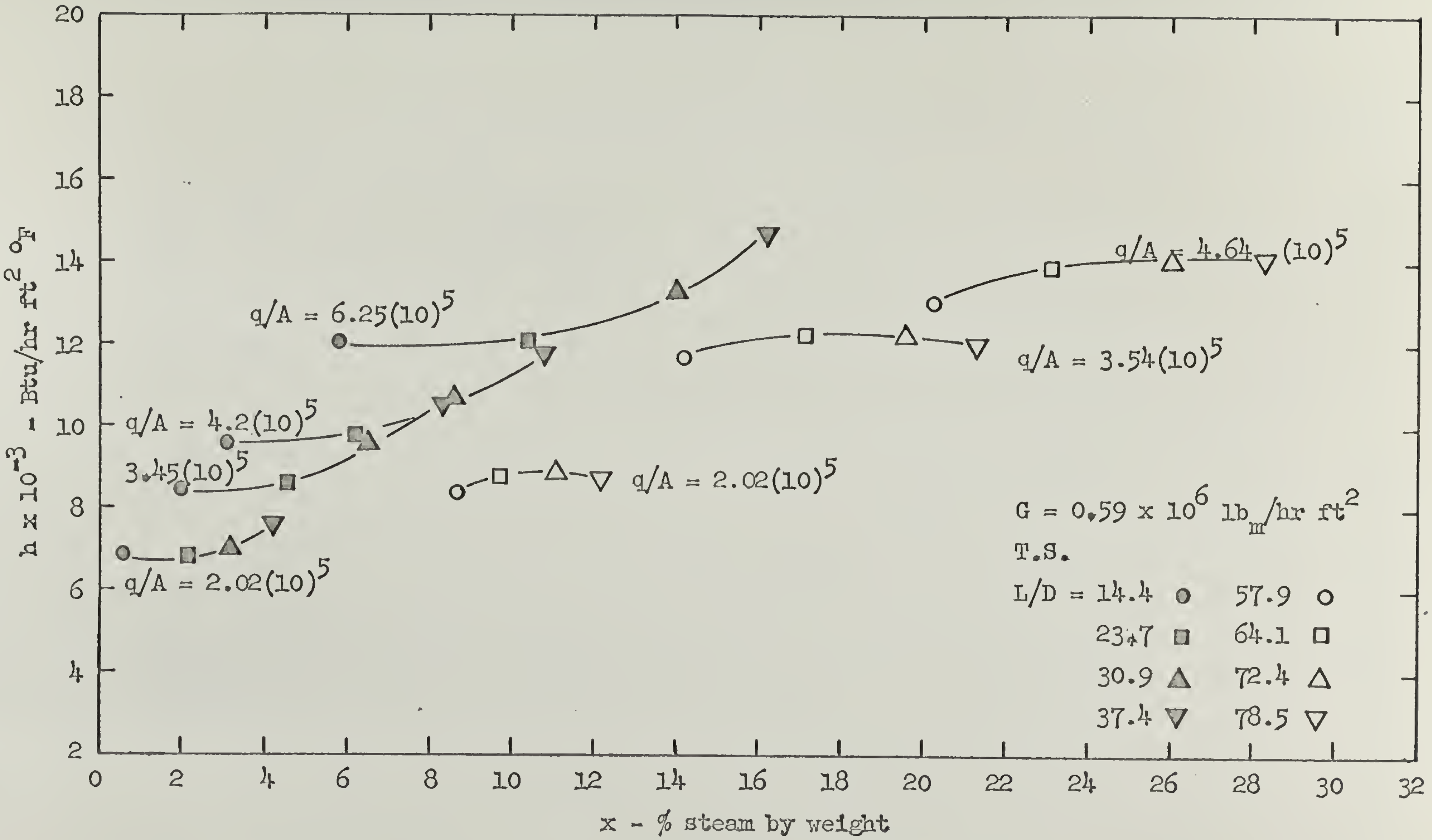

FIG. 13 COMPARISON OF HEAT TRANSFER COEFFICIENT FOR T.S. 2 AND 3.

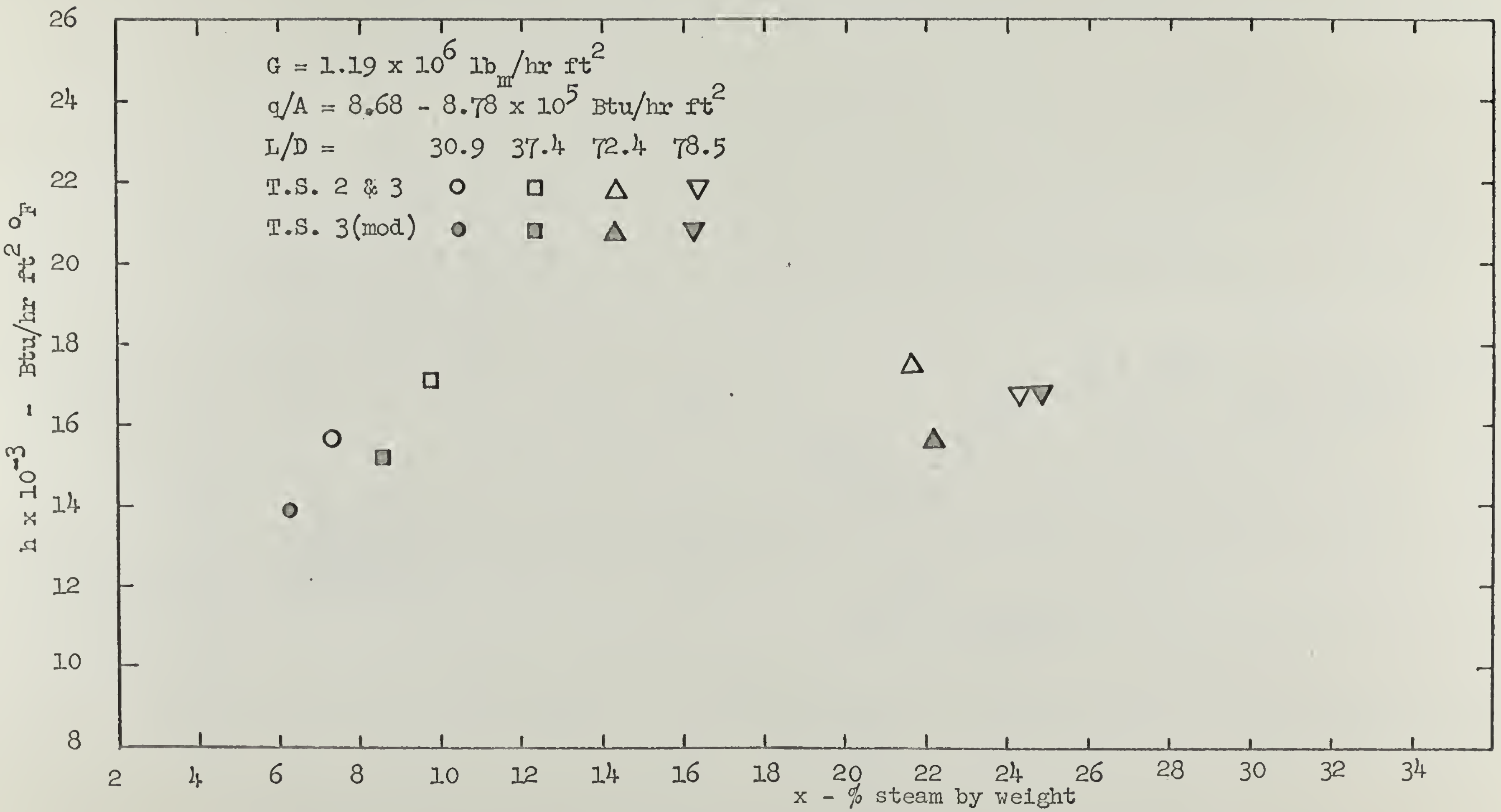

FIG. 14 COMPARISON OF HEAT TRANSFER COEFFICIENT FOR T.S. 2, 3, AND 3 MODIFIED.

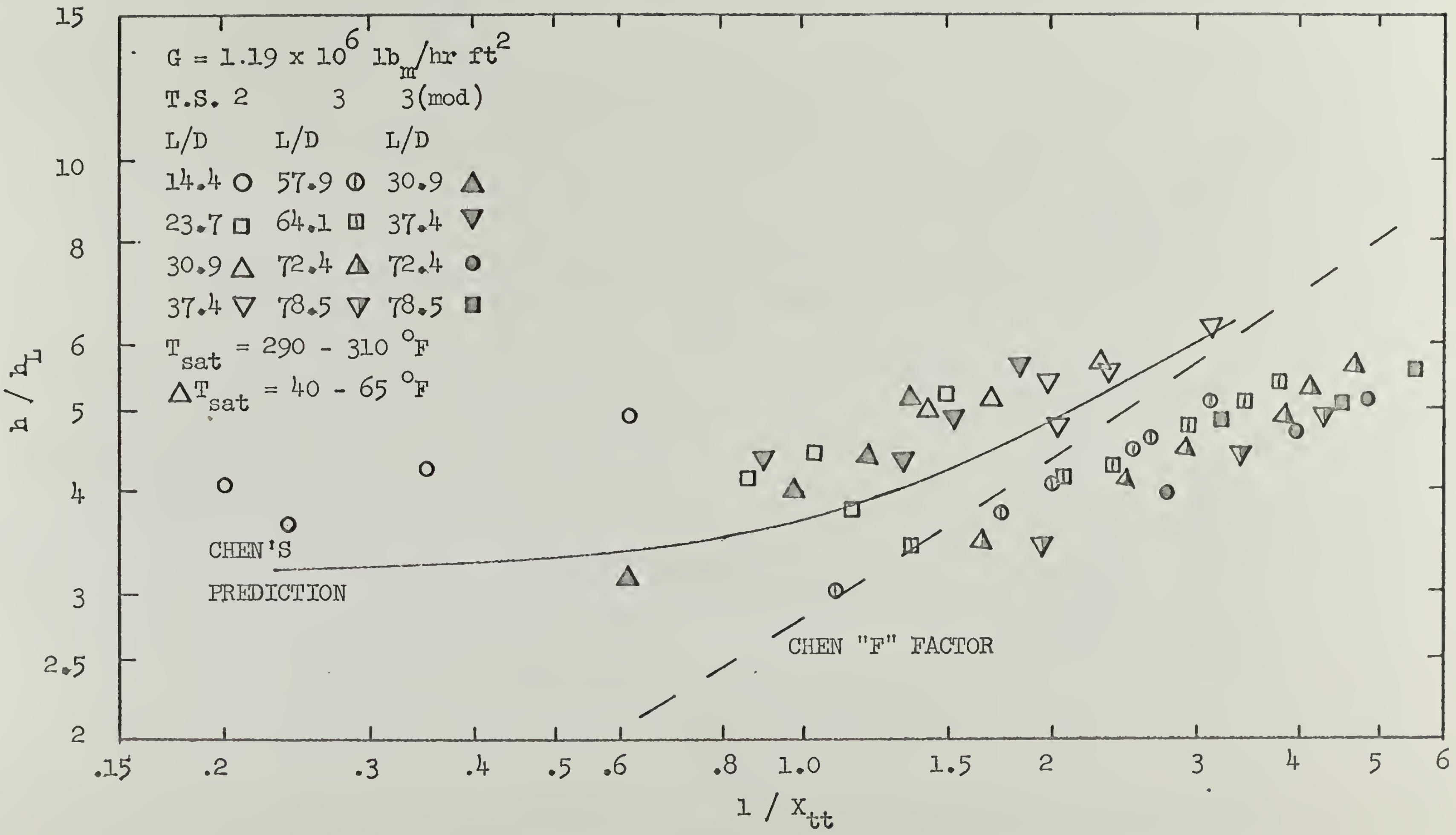

FIG. 15 CORRELATION OF HEAT TRANSFER COEFFICIENT FOR T.S. 2, 3, AND 3 MODIFIED.

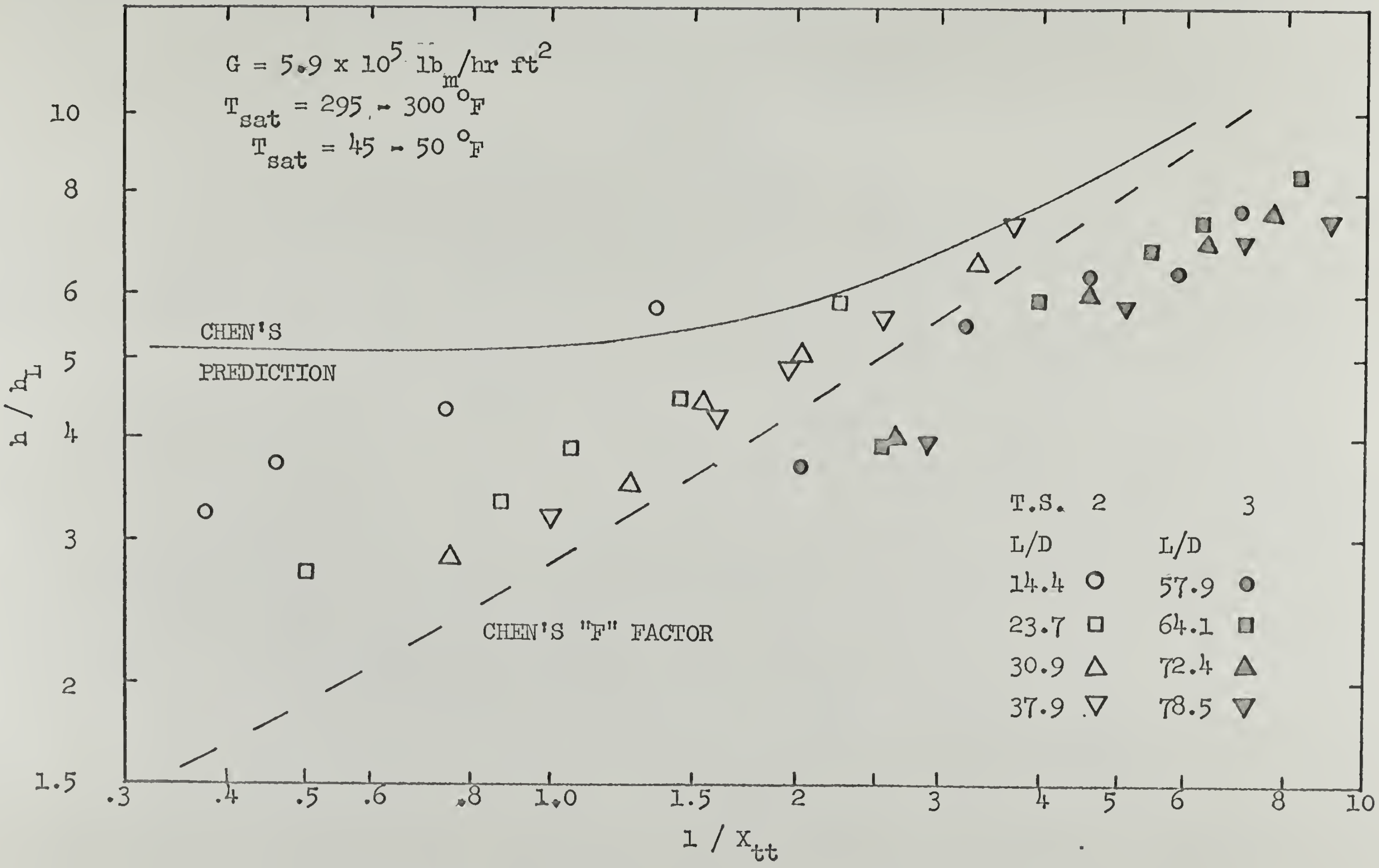

FIG. 16 CORRELATION OF HEAT TRANSFER COEFFICIENT FOR T.S. 2, AND 3.